Available online at www.sciencedirect.com
SCIENCE DIRECT®
Developmental Biology 290 (2006) 220 – 235
DEVELOPMENTAL BIOLOGY
www.elsevier.com/locate/ydbio

Sperm capacitation induces an increase in lipid rafts having zona pellucida binding ability and containing sulfogalactosylglycerolipid

Maroun Bou Khalil [a,b], Krittalak Chakrabandhu [a], Hongbin Xu [a,b], Wattana Weerachatyanukul [a], Mary Buhr [c], Trish Berger [d], Euridice Carmona [a], Ngoc Vuong [a,b], Premkumari Kumarathasan [e], Patrick T.T. Wong [b], Danielle Carrier [b], Nongnuj Tanphaichitr [a,b,f,*]

[a] *Hormones/Growth/Development Group, Ottawa Health Research Institute, Ottawa, ON, Canada K1Y 4E9*
[b] *Department of Biochemistry/Microbiology/Immunology, University of Ottawa, Ottawa, ON, Canada K1H 8M5*
[c] *Department of Animal and Poultry Science, University of Guelph, Guelph, ON, Canada N16 2W1*
[d] *Department of Animal Science, University of California, Davis, CA 95616, USA*
[e] *Environmental Health Sciences Bureau, Health Canada, Tunney's Pasture, Ottawa, ON, Canada K1A 0L2*
[f] *Department of Obstetrics/Gynecology, University of Ottawa, ON, Canada K1H 8M5*

Received for publication 17 April 2005, revised 10 November 2005, accepted 15 November 2005
Available online 4 January 2006

Abstract

Sperm gain full ability to bind to the zona(e) pellucida(e) (ZP) during capacitation. Since lipid rafts are implicated in cell adhesion, we determined whether capacitated sperm lipid rafts had affinity for the ZP. We demonstrated that lipid rafts, isolated as low-density detergent resistant membranes (DRMs), from capacitated pig sperm had ability to bind to homologous ZP. This binding was dependent on pig ZPB glycoprotein, a major participant in sperm binding. Capacitated sperm DRMs were also enriched in the male germ cell specific sulfogalactosylglycerolipid (SGG), which contributed to DRMs-ZP binding. Furthermore, SGG may participate in the formation of sperm DRMs due to its interaction with cholesterol, an integral component of lipid rafts, as shown by infrared spectroscopic studies. Since sperm capacitation is associated with cholesterol efflux from the sperm membrane, we questioned whether the formation of DRMs was compromised in capacitated sperm. Our studies indeed revealed that capacitation induced increased levels of sperm DRMs, with an enhanced ZP affinity. These results corroborated the implication of lipid rafts and SGG in cell adhesion and strongly suggested that the enhanced ZP binding ability of capacitated sperm may be attributed to increased levels and a greater ZP affinity of lipid rafts in the sperm plasma membrane.

Keywords: Sperm; Sperm capacitation; Lipid rafts; Detergent resistant membranes; Sulfogalactosylglycerolipid; Cholesterol; Zona pellucida

Introduction

Capacitation is a process occurring in the female reproductive tract during which mammalian sperm acquire full fertilizing ability. During capacitation, albumin and high-density lipoproteins, present in the female reproductive tract (Flesch et al., 2001a; Wolf et al., 1986; Visconti et al., 2002), induce the release/efflux of cholesterol from the sperm plasma membrane. Since sperm cells also possess a substantial amount of glycerophospholipids containing polyunsaturated fatty acids (PUFA) (Parks and Lynch, 1992; Nikolopoulou et al., 1985), cholesterol efflux leads to a global increase in membrane fluidity in capacitated sperm, which is beneficial to the fusion-related events during sperm–egg interaction, i.e., the zona pellucida (ZP)-induced sperm acrosome reaction and the sperm–egg plasma membrane fusion (Primakoff and Myles, 2002). However, the initial interaction between sperm and eggs, i.e., the sperm–ZP binding, would likely require ordered microdomains on the sperm plasma membrane with clusters of ZP binding molecules, as the interaction has to be stable enough to withstand the pulling force generated from ongoing sperm movement (Baltz et al., 1988). In addition, it would be advantageous to have signaling molecules together with ZP binding molecules in the same ordered microdomains

* Corresponding author. Ottawa Health Research Institute, 725 Parkdale Ave., Ottawa, ON, Canada K1Y 4E9. Fax: +1 613 761 5365.
E-mail address: ntanphaichitr@ohri.ca (N. Tanphaichitr).

0012-1606/$ - see front matter © 2005 Elsevier Inc. All rights reserved.
doi:10.1016/j.ydbio.2005.11.030

for an immediate onset of the subsequent sperm signaling events.

Accumulating evidence reveals that cellular membranes in somatic cells contain liquid-ordered microdomains, termed lipid rafts, which are enriched in cholesterol, sphingomyelin (SM), glycosphingolipids and saturated phospholipids (Brown and London, 2000; Simons and Vaz, 2004). The interaction between cholesterol and other raft lipids is crucial for the formation of liquid-ordered microdomains, segregated from the remaining more fluid membrane (Silvius, 2003; Simons and Vaz, 2004). Lipid rafts can be isolated as membrane vesicles that are resistant to non-ionic detergents at low temperatures (Schuck et al., 2003). Certain raft lipid components in somatic cells, such as monosialogangliosides–GM1 and GM3, are involved in cell adhesion and signaling (Marmor and Julius, 2001; Iwabuchi et al., 2000; Nagafuku et al., 2003). In addition, numerous proteins involved in cell adhesion and signaling are found in lipid rafts isolated from somatic cells (Foster et al., 2003; Moffett et al., 2000; Galbiati et al., 2001; Harris and Siu, 2002). Therefore, lipid rafts are implicated as platforms of cell adhesion and signaling molecules (Simons and Ehehalt, 2002; Brown and London, 2000; Hakomori, 2000; Horejsi, 2003), and isolated lipid rafts would be ideal cell-free systems for studying integrative mechanisms of cell–cell interaction and signal transduction events. While lipid rafts isolated from gametes would be suitable for these studies, reports on gamete lipid rafts, especially those of the mammalian system, are still limited. To date, sea urchin sperm DRMs have been shown to have an affinity for a 350-kDa sperm binding protein (SBP) of the egg vitelline layer. These sea urchin sperm DRMs are enriched in sialylated gangliosides and sulfogalactosylceramide (SGC, [β-D-(3′-sulfatoxy)galactopyranosyl]-1′-1-*N*-tetracosanoylsphingosine), which play a significant role in egg binding (Maehashi et al., 2003; Ohta et al., 1999). *Xenopus* egg DRMs are also implicated in sperm-induced signaling events (Sato et al., 2002, 2003). DRMs have been isolated from mammalian sperm (Travis et al., 2001; Nishimura et al., 2001; Cross, 2004; Shadan et al., 2004; Sleight et al., 2005; van Gestel et al., 2005) and a few reports indicate existence of proteins with affinity for the ZP and egg plasma membrane in sperm DRMs (Nishimura et al., 2001; Sleight et al., 2005; van Gestel et al., 2005). However, the direct binding of sperm DRMs to these egg entities is yet to be demonstrated. In addition, since the efflux of cholesterol (an integral component of lipid rafts) is associated with mammalian sperm capacitation, it is important to determine whether the formation of lipid rafts is compromised in capacitated sperm.

Mammalian sperm have a few unique features on their lipid composition. Besides possessing PUFA-glycerophospholipids, mammalian sperm selectively contain sulfogalactosylglycerolipid (SGG, 1-*O*-hexadecanyl-2-*O*-hexadecanoyl-[β-D-(3′-sulfatoxy)galactopyranosyl(1′–3)]-*sn*-glycerol, also known as seminolipid). SGG constitutes ~5–10 mol% of total sperm lipids (Tanphaichitr et al., 2003). Model membrane studies indicate a high phase transition temperature (45°C) of SGG due to the saturated nature of its hydrocarbon chains (16:0/16:0), as well as strong intermolecular hydrogen bonding networks among SGG molecules, resulting in the formation of ordered crystal-like SGG bilayers (Attar et al., 2000). There is also evidence that SGG is involved in sperm–ZP binding (White et al., 2000; Weerachatyanukul et al., 2001), and it is a structural analog of SGC, found in sea urchin sperm DRMs. With all of these properties of SGG, we launched our efforts to determine whether SGG is a component of sperm DRMs and whether SGG participates in the binding of sperm DRMs to the egg ZP.

Materials and methods

SGG and affinity purified anti-SGG IgG/Fab were prepared as previously described (Tupper et al., 1994; White et al., 2000). Dipalmitoylglycerophosphorylcholine (DPPC) was purchased from Avanti Polar Lipids (Alabaster, AL, USA). Phospholipid standards (porcine liver glycerophosphorylcholine (PC), glycerophosphorylethanolamine (PE), and bovine brain SM) were from Doosan Serdary Research Laboratories (Englewood Cliffs, NJ, USA). Cholesterol and fatty acid free bovine serum albumin (BSA) were from Sigma (St. Louis, MO, USA). Triton X-100 was from Bio-Rad Laboratories (Hercules, CA, USA). Alexa 430 was purchased from Molecular Probes (Eugene, OR, USA).

Pig sperm preparation and capacitation

Ejaculated semen samples collected from mature fertile boars were diluted in Beltsville Thawing Solution (BTS: 0.2 M glucose, 20 mM sodium citrate, 15 mM $NaHCO_3$, 3.36 mM Na_2EDTA, 10 mM KCl, 8 mM Na_2HPO_4, 2 mM NaH_2PO_4, and 1 mg/ml dihydrostreptomycin, pH 7.4) and stored (18°C, <24 h) in dark until use. Sperm, washed free of seminal plasma by centrifugation (350 × *g*, 28°C, 10 min), were resuspended at 1×10^9 sperm/ml in non-capacitation medium (NCM: 0.1 M NaCl, 0.36 mM NaH_2PO_4, 8.6 mM KCl, 0.5 mM $MgCl_2$, 11 mM glucose, 23 mM HEPES, pH 7.6) (Melendrez et al., 1994). Motile sperm populations were prepared by density gradient (35% and 70% Percoll diluted in NCM) centrifugation (600 × *g*, 28°C, 30 min) (Harrison et al., 1993) and resuspended to a final concentration of 10×10^6 sperm/ml in either NCM or capacitation medium (CM: containing all components of NCM plus 10 mM $NaHCO_3$, 2 mM $CaCl_2$, 5 mM pyruvate and 0.3% BSA (Melendrez et al., 1994)). More than 90% of these sperm were motile as assessed microscopically. About 10–15% of sperm resuspended in NCM readily attained hyperactivated motility patterns, suggesting that Percoll gradient centrifugation could induce a low level of capacitation. In contrast, more than 90% of sperm incubated (3 h, 39°C, 5% CO_2), in CM possessed hyperactivated motility patterns and other properties (see Results and Fig. 1) typical of capacitated sperm (Visconti et al., 2002; Flesch et al., 2001a,b; Yanagimachi, 1994). Therefore, these sperm were referred to as "capacitated sperm", whereas sperm resuspended in NCM served as a control in all capacitation-related studies.

Cholesterol staining in live control and capacitated sperm

Control and capacitated sperm (1×10^6 sperm/ml) resuspended in NCM were incubated (37°C, 30 min) with 25 μM filipin (Sigma; made as a 10-mM stock solution in dimethylsulfoxide (DMSO)), which binds specifically to cholesterol (Friend, 1982). Sperm were washed free of unbound filipin by low speed centrifugation in NCM, and viewed under a Zeiss IM35 epifluorescent microscope using a Hoechst filter (excitation and emission wavelength of 365 and 420 nm, respectively). Approximately 200 sperm in each sample were examined for the fluorescence staining pattern and intensity.

Sperm tyrosine phosphorylation in control and capacitated sperm

One million control and capacitated sperm were separately treated with SDS-PAGE sample buffer at 94°C for 5 min. After centrifugation at 14,000 × *g* for 5 min, the supernatant was subjected to SDS-PAGE (12% polyacrylamide gel), followed by immunoblotting as previously described (Laemmli, 1970; Towbin and Gordon, 1984). Tyrosine phosphorylated proteins were detected

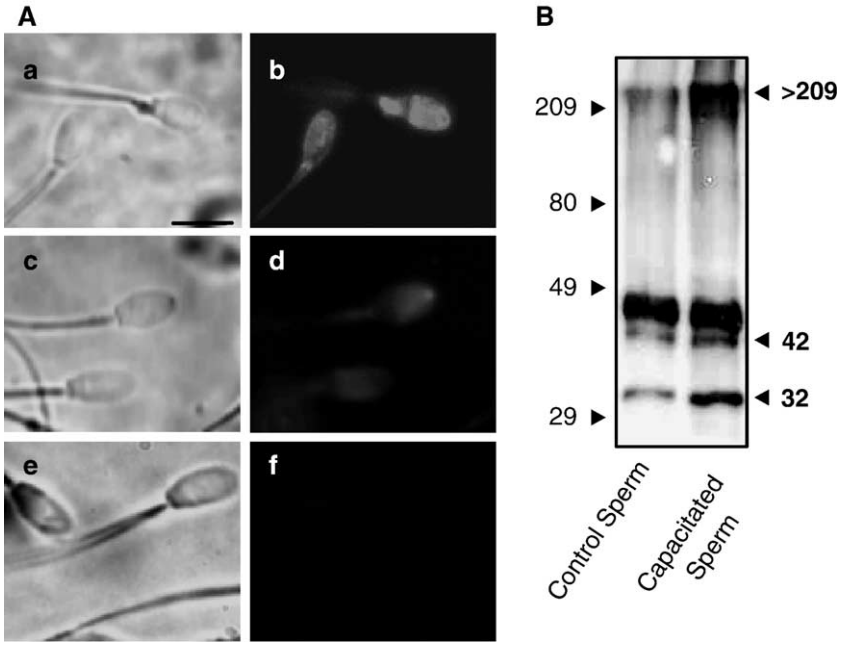

Fig. 1. Decreased cholesterol content and increased sperm tyrosine phosphorylation in capacitated pig sperm. (A) Filipin staining of live control sperm (a, b) and capacitated sperm (c, d). Control sperm treated with DMSO were shown in panels e and f. Panels a, c and e: phase contrast micrographs; panels b, d and f: corresponding fluorescent images. Scale bar = 10 μm. (B) Sperm tyrosine phosphorylation. An equal number of control and capacitated sperm (1×10^6) was used for immunoblotting with monoclonal IgG antibody 4G10. Arrowheads on the right side mark an increase in the immunoreactivity of the >209 kDa, 42 kDa and 32 kDa bands. Positions of molecular weight standards (in kDa) are marked by arrowheads on the left side of the panel. Results shown are representative of 3 replicate experiments performed on different days.

using a mouse monoclonal IgG antibody 4G10 (Upstate, Waltham, MA, used at 2 μg/ml) that specifically recognizes phosphotyrosine. Antigen–antibody recognition was detected using HRP-conjugated goat anti-mouse IgG antibody (Bio-Rad Laboratories, 1:20,000 dilution) and an ECL Western blotting detection kit (Amersham Pharmacia Biotech, Piscataway, NJ). Tris-buffered saline (TBS, 20 mM Tris–HCl, 137 mM NaCl, pH 7.4) containing 5% non-fat powdered milk was used for diluting antibodies and blocking non-specific binding to nitrocellulose membrane.

Preparation of sperm head anterior plasma membranes (APMs)

Capacitated pig sperm were resuspended at 1×10^9 sperm/ml in 1 mM Tris–HCl, pH 7.4 containing 0.25 M sucrose, and their APMs were selectively extracted by nitrogen cavitation using a Parr cell disruptor (Parr Instrument Company, Moline, IL) at 650 psi (Peterson et al., 1980). Following low speed centrifugation to pellet sperm particulates, APM vesicles in the supernatant were collected and then subjected to ultracentrifugation (117,730 × *g*, 4°C, 90 min) in a 70 Ti rotor (Beckman, Palo Alto, CA, USA). The APMs pellet was then resuspended in a small volume of TBS and kept frozen until use for the ZP binding assay (see below).

Preparation of sperm tails

Capacitated sperm resuspended in TBS were sonicated (Fisher Sonic Dismembrator, Model 300, 30% intensity, 2 min) to dissociate tails from heads. The sonicated sperm suspension was washed twice with TBS, resuspended in TBS containing 80% (w/v) sucrose and ultracentrifuged (280,000 × *g*, 4°C, 1 h) using a 70 Ti rotor (Shao et al., 1997). The sperm tails, pelletted on the inner side of the tube, were collected and further purified by ultracentrifugation through a 40%/60%/80% TBS-containing sucrose gradient on a horizontal rotor (100,000 × *g*, 4°C, 1 h). The pure sperm tail fraction was obtained from the 60%/80% sucrose interface and washed twice in TBS by centrifugation (8000 × *g*, 4°C, 30 min). The isolated sperm tails were unbroken, although some degree of plasma membrane disruption was observed by electron microscopy as previously described (Shao et al., 1997). These pure unbroken sperm tails were used for DRMs isolation.

Immunofluorescence of SGG in control and capacitated sperm

This was performed with fixed and live sperm at ~1×10^7 sperm/ml. For the fixed sperm, control and capacitated sperm were first washed with PBS and then treated (20 min, room temperature) with 4% paraformaldehyde in PBS. After washing twice with PBS, excess aldehyde was removed from the fixed sperm by exposure to 0.2 M glycine in PBS (15 min, room temperature). Sperm were then blocked against non-specific binding with 5% goat serum in PBS (30 min, room temperature), and treated (1 h, room temperature) with 2 μg/ml affinity purified anti-SGG IgG followed by 4 μg/ml Alexa-488 goat anti-rabbit IgG (Molecular Probes). Sperm were washed twice with PBS after antibody incubation, mounted onto a slide and topped with a coverslip for microscopic imaging. Live control and capacitated sperm were processed in the same manner as fixed sperm except that the aldehyde and glycine treatment steps were omitted. To evaluate the specificity of the antibody, anti-SGG IgG preadsorbed with 10× excess of SGG multilamellar liposomes (prepared as described below) was also used for sperm staining. Sperm slides were viewed under a Bio-Rad MRC-1024 Laser Scanning Confocal Microscope equipped with an argon ion laser and mounted on an Olympus IX70 inverted microscope. An Olympus Plan-Apo 60× objective (N.A. 1.4) was used for imaging. Alexa-488 fluorescence was captured with the slow scanning mode using a fluorescein filter set. SGG globular units observed in immunofluorescent images of both fixed and live sperm were analyzed for their size using Image J1.27z program downloaded from http://rsb.info.nih.gov/ij/.

Isolation of sperm lipid rafts

Lipid rafts were isolated from control sperm, capacitated sperm, and sperm tails as low-density DRMs according to the described method (Brown and Rose, 1992). Sperm were resuspended at 1×10^9 sperm/ml in the prechilled (4°C) lysis buffer (TNE: 10 mM Tris–HCl, 0.15 M NaCl, and 5 mM EDTA, pH 7.5) containing 1% Triton X-100 and 0.2 mM TLCK (*N*-α-*p*-tosyl-L-lysine

chloromethyl ketone). This ratio of the number of sperm to the amount of Triton X-100 was chosen based on our pilot studies, which indicated the highest yield of lipid rafts obtained from both control and capacitated sperm. Notably, a similar ratio was used for human sperm (Cross, 2004). When this ratio was converted to the weight ratio of cellular proteins to Triton X-100, it appeared to be similar to that described for the maximum low-density DRM isolation in human leukemia cells (Panasiewicz et al., 2003). Following addition of the lysis buffer to the pig sperm suspension, the mixture was kept on ice for 1 h, and then homogenized by 30 strokes in a Dounce homogenizer. After pelleting sperm by centrifugation (1300 × *g*, 4°C, 10 min), the supernatant (lysate) was mixed with an equal volume of 85% (w/v) sucrose in TNE. Two ml of the lysate in 42.5% (w/v) sucrose-TNE was placed in each ultracentrifuge tube, and overlaid with 6 ml of 30% sucrose-TNE and 3.5 ml of 5% sucrose-TNE. The tubes were ultracentrifuged (200,000 × *g*, 18 h, 4°C) using a SW 40 Ti rotor (Beckman), and 1-ml fractions were collected from top to bottom and measured for their light scattering intensity at A_{400} (Xu et al., 2001). Each fraction was also analyzed for protein content using Bio-Rad Protein Assay and cholesterol content by the Amplex Red fluorometric assay (as described by Molecular Probes). Three to five replicates of each fraction were used in cholesterol and protein assays. Low-density DRM fractions (#4 to 6, as shown in Fig. 3), having high A_{400}, were pooled and ultracentrifuged (285,000 × *g*, 4°C, 70 min) in a 70 Ti rotor (Beckman). The pelleted DRMs were used for lipid extraction and evaluation of their ZP binding ability.

SDS-PAGE and immunoblotting of sucrose gradient fractions

An equal volume of each fraction from the sucrose density gradient of the sperm Triton X-100 lysate was subjected to SDS-PAGE (12% polyacrylamide gel), followed by immunoblotting with mouse monoclonal antibody against flotillin-2 (BD Biosciences, San Jose, CA, USA, 1:1000 dilution). Antigen–antibody recognition was detected by ECL using HRP-conjugated goat anti-mouse IgG antibody (Bio-Rad Laboratories, 1:2000 dilution).

Lipid analyses

For cholesterol and phospholipid quantification, sperm and isolated DRMs were stored at −20°C in glass vials, flushed with N_2 stream and closed tightly with screw caps. For other lipid work, sperm and DRMs were stored frozen in the presence of antioxidants, 0.02 M diethylenetriaminepentaacetic acid + 0.06 M butylated hydroxytoluene. Lipids were extracted from these biological materials as described (Furimsky et al., 2005). Cholesterol in the isolated lipids was quantified by the Amplex Red assay (sensitivity of 0.1 μg), as described above. Phospholipids and SGG in the same lipid samples were quantified by colorimetric assays (Duck-Chong, 1979; Kean, 1968) with a sensitivity of 0.02 μg and 1 μg, respectively. Three replicates of each sample were used for all quantitative lipid analyses on each experimental day. To calculate the amounts of these three lipid classes in each sperm/DRMs sample, known molecular masses of cholesterol (387 Da) and the major molecular species of SGG (796 Da), and an average molecular mass of phospholipids (750 Da) were used.

Lipids from sperm and isolated DRMs were also characterized by high performance thin layer chromatography (HPTLC) (White et al., 2000), using chloroform/methanol/water (65:32:4, v/v/v) as the solvent system. To compare the ratio of SGG to phospholipids (PC, PE and SM) in sperm DRMs with that in whole sperm, the amounts of lipid samples applied onto the plate were adjusted, so that the same amount of SGG (i.e., 3 μg) was present in all samples. Chromatographed lipids were stained with 0.03% Coomassie blue G-250 in 30% methanol/100 mM NaCl, and the distribution of PC, PE and SM was analyzed densitometrically (Furimsky et al., 2005). The amounts of PC + PE and SM were calculated based on this distribution and the amounts of total phospholipids determined as described above, assuming that PC + PE + SM (the major subclasses) constituted 100% of total phospholipids. The hydrocarbon chains of PC and PE from control and capacitated sperm DRMs were characterized by subjecting these phospholipid subclasses, purified by preparative thin layer chromatography, to acid methanolysis (Kates et al., 1986) to generate fatty acid methyl esters (FAMEs) from ester phospholipids and dimethylacetals (DMAs) from plasmalogens. Identities of FAMEs and DMAs were analyzed by gas chromatography/mass spectrometry (Furimsky et al., 2005).

Fourier transform infrared (FTIR) spectroscopy

Multilamellar bilayers of equimolar mixtures of SGG-cholesterol and DPPC-cholesterol were generated as 5% by weight dispersions in ^2H_2O buffered with 50 mM Tris–HCl (p^2H 7.05), and subjected to four freeze–thaw cycles (Bou Khalil et al., 2001). FTIR spectroscopic measurements and data processing were conducted following our described procedures (Bou Khalil et al., 2001). Hydrogen bonding interactions of SGG and DPPC with cholesterol were monitored using the ester carbonyl stretching band (from 1700 to 1760 cm^{-1}). The free (non-hydrogen bonded) and hydrogen-bonded ester carbonyl species gave an absorbance peak at ~1740 cm^{-1} and ~1720 cm^{-1}, respectively (Wong and Mantsch, 1988).

Binding of pig sperm DRMs and APMs to solubilized homologous ZP

The interaction of isolated pig sperm DRMs and APMs with solubilized Alexa-430 conjugated pig ovarian ZP (Alexa-430 ZP) was investigated using a microwell binding assay. Solubilized ovarian ZP, prepared as previously described (Hedrick and Wardrip, 1987), were conjugated to Alexa 430 following instructions from Molecular Probes. Total proteins in sperm DRMs and APMs were quantified using Bio-Rad Protein Assay Solution. Sperm DRMs and APMs were resuspended in 100 mM sodium carbonate, pH 9.6; 100 μl of the DRMs or APMs suspension containing 0.5 μg protein was coated in each well of a black polystyrene 96-well microtiter plate (Corning Inc., New York, NY, USA) at 4°C for 24 h. After blocking (1 h, at room temperature) with 1% BSA in TBS, the DRMs or APMs in the wells were washed three times with TBS, and incubated (1 h, room temperature) with 0 to 0.4 μM of Alexa-430 ZP in 100 μl TBS. Following three successive washes with TBS to remove unbound Alexa-430 ZP, fluorescence intensity of each well was measured

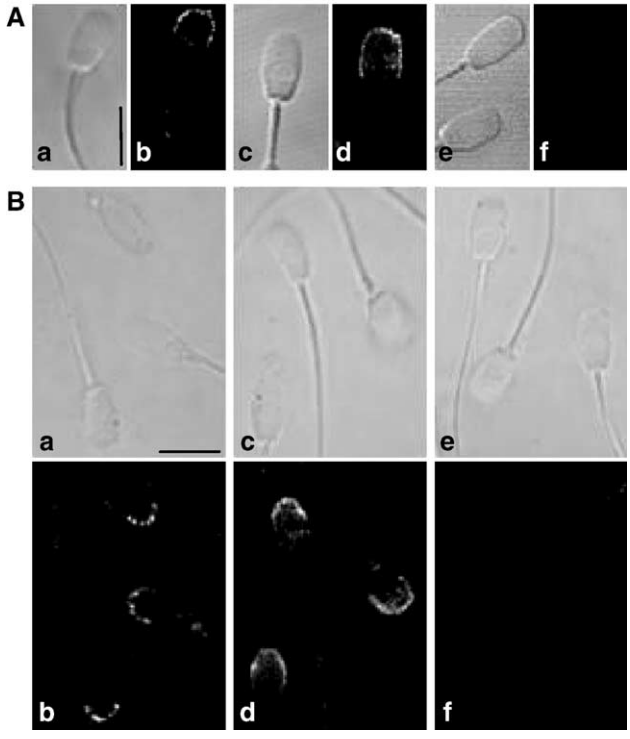

Fig. 2. Immunolocalization of SGG in pig sperm. (A) aldehyde fixed sperm; (B) live sperm. Control sperm (a, b) and capacitated sperm (c, d) were incubated with affinity purified anti-SGG IgG and then Alexa-488 secondary antibody. Panels e and f display capacitated sperm that were incubated with preimmune rabbit serum IgG instead of anti-SGG IgG. In both (A) and (B), panels a, c and e: phase contrast micrographs; panels b, d and f: corresponding fluorescent images. Scale bar = 10 μm. Results shown are representative of 3 replicate experiments performed on different days.

spectrofluorometrically at excitation and emission wavelength of 425 and 520 nm, respectively. The amount of Alexa-430 ZP bound to sperm DRMs/APMs was determined from the Alexa-430 ZP standard curve. Three replicates of each sperm DRMs sample and APMs sample were used for protein analyses and binding assays for each Alexa-430 ZP concentration, performed on each experimental day.

The dissociation constant (K_d) and maximum binding capacity (B_{max}) of Alexa-430 ZP to sperm DRMs/APMs were determined after subtracting non-specific binding levels of the Alexa-430 ZP ligand from its total binding levels to DRMs/APMs. Non-specific binding levels were determined by including unlabeled solubilized ZP (at a 100-fold excess of Alexa-430 ZP) in the co-incubates of Alexa-430 ZP and sperm DRMs or APMs. The K_d and B_{max} of DRMs/APMs-ZP binding were calculated by non-linear regression using GraFit 4.09 software for Windows (Erithacus Software Ltd., Horley, Surrey, U.K.).

To further determine whether the interaction between sperm DRMs and Alexa-430 ZP was specific, Alexa-430 ovalbumin (produced in the same manner as Alexa-430 ZP, and known for its inability to bind to intact sperm (Carmona et al., 2002b)) was used as the binding ligand instead of Alexa-430 ZP. In addition, since sperm tails do not have an affinity for ZP (Yanagimachi, 1994), isolated pig sperm tail DRMs were used in place of whole sperm DRMs for incubation with Alexa-430 ZP.

To investigate whether the binding of capacitated sperm DRMs to Alexa-430 ZP was dependent on total and individual pig ZP glycoproteins, competitive binding assays were performed by including various amounts of ZP glycoproteins in the DRMs-Alexa-430 ZP co-incubates. ZP glycoproteins used as competitors included pig ZP(B + C), ZPB and ZPC, also known as pig ZP3, ZP3α and ZP3β, respectively. ZP(B + C) was purified from solubilized pig ZP, and ZPB and ZPC (both slightly deglycosylated) were prepared from endo-β-galactosidase treated ZP(B + C) (Yurewicz et al., 1987). All of these pig ZP glycoproteins were provided by Dr. E. Yurewicz (Wayne State University, Detroit, MI, USA). Solubilized whole pig ZP and ZP polypeptide cores, prepared by deglycosylating solubilized pig ZP with trifluoromethanesulfonic (TFMS) (Hedrick and Wardrip, 1987), were also used as competitors. Alexa-430 ZP (0.2 μM) was incubated with capacitated sperm DRMs (attached to the microtiter plate wells) in the presence of 0 to 4 μM of each competitor. Molarity of ZP(B + C), solubilized whole ZP and ZP polypeptides were calculated as previously described (Carmona et al., 2002a). The levels of Alexa-430 ZP binding to sperm DRMs were expressed as percentages of the value obtained from the control conditions, i.e., in the absence of competitor ZP glycoproteins in the co-incubates. Ovalbumin in the same concentration range as pig ZP glycoproteins was used as a negative control in these competitive binding assays.

Participation of SGG in sperm DRMs-ZP binding was also evaluated. Capacitated sperm DRMs immobilized in the microtiter wells were pretreated (1 h, room temperature) with 0 to 16 μM affinity purified anti-SGG IgG or Fab. These concentration ranges gave antigen-binding units corresponding to 0.5 to 2 fold SGG present in sperm DRMs in each well. The DRMs-coated wells were washed three times with TBS to remove unbound antibody, and then assessed for binding to 0.2 μM Alexa-430 ZP. In alternate experiments, capacitated sperm DRMs were pretreated with preimmune rabbit serum IgG/Fab instead of anti-SGG IgG/Fab. The binding levels of Alexa-430 ZP to sperm DRMs pretreated with antibody were expressed as percentages of the value obtained from untreated DRMs.

Binding of SGG-containing liposomes to solubilized pig ZP

Multilamellar bilayers containing SGG, cholesterol and a model saturated phospholipid, DPPC, were generated in TBS, as described above. The molar ratio of SGG, cholesterol and DPPC used in this liposome preparation was 1.0:2.0:3.4, mimicking that of these three lipid classes in isolated capacitated sperm DRMs (see Results). SGG-depleted liposomes, containing only cholesterol and DPPC (molar ratio: 2.0:3.4), were also generated. Both types of liposomes (2 μg/assay tube) were preblocked for non-specific binding with 1% BSA in TBS (1 h, room temperature). After ultracentrifugation (100,000 × *g*, 4°C, 1 h), the liposomes were incubated (1 h, 37°C) with 0 to 0.4 μM of Alexa-430 ZP in 100 μl TBS. To determine the levels of non-specific binding of Alexa-430 ZP, SGG-containing liposomes were incubated with Alexa-430 ZP + 100-fold excess of unlabeled ZP. After the incubation, the liposomes were ultracentrifuged (100,000 × *g*, 4°C, 1 h) to remove unbound Alexa-430 ZP. The resulting pellet (Alexa-430 ZP–liposome complexes) was resuspended in 100 μl TBS and fluorescence intensity of the suspension was measured spectrofluorometrically.

Statistical analyses

Student's *t* test and ANOVA were used to determine significant differences between two data sets.

Results

Properties of capacitated pig sperm

Fig. 1A demonstrates that both capacitated sperm and control sperm were mainly stained with filipin in the head region. However, capacitated sperm had lower fluorescence staining intensity than control sperm, suggesting that cholesterol levels were reduced following capacitation. This result was confirmed by biochemical analysis of cholesterol (see below). Capacitated sperm also showed higher levels of sperm tyrosine phosphorylation. Immunoblotting of both control and capacitated sperm with 4G10 monoclonal antibody indicated tyrosine phosphorylated proteins bands of molecular masses of >209 kDa, 45 kDa, 42 kDa and 32 kDa (Fig. 1B). Except for the 45-kDa band, the immunoreactive intensity of the other three bands was higher in capacitated sperm, indicating that they had higher levels of protein tyrosine phosphorylation than control sperm. The observation on the higher tyrosine phosphorylation level of the 32-kDa band in capacitated pig sperm was in accordance with previously described results (Tardiff et al., 2001; Flesch et al., 1999; Shadan et al., 2004). However, the increased tyrosine phosphorylation of the 42-kDa and >209-kDa bands is reported here for the first time.

Localization of SGG to the sperm head surface

Indirect immunofluorescence of live pig sperm revealed that SGG was localized exclusively to the sperm head surface (Fig. 2), the site of ZP interaction (Burkin and Miller, 2000). In approximately 75% of aldehyde-fixed and live control sperm, the SGG fluorescent staining appeared as dot-like patterns, with the same average size of 0.5 μm (range: 0.47 to 0.60 μm for fixed sperm and 0.36 to 0.72 μm for live sperm, $n = 20$ for each sperm sample). SGG was confined to the anterior periphery of the head in both fixed and live control sperm samples (fixed sperm: Fig. 2A—panels a, b; live sperm: Fig. 2B—panels a, b). In contrast, SGG staining in fixed and live capacitated sperm was observed not only at the anterior periphery of the head but also posteriorly in the acrosomal region, although the staining intensity was still highest in the head anterior edge (fixed sperm: Fig. 2A—panels c, d; live sperm: Fig. 2B—panels c, d). The sizes of the globular fluorescent patterns in capacitated sperm were the same as those in control sperm. However, in live capacitated sperm, these globular units appeared to be more connected with each other than in live control sperm (Fig. 2B, panel d versus panel b). About 25% of live and fixed sperm (both control and

capacitated) did not show any immunofluorescent staining with anti-SGG IgG. This may reflect the sperm population that was not viable (positive staining with propidium iodide, about 15% of total sperm) and acrosome reacted sperm (about 10% of total sperm) (data not shown). Sperm exposed to preimmune rabbit serum IgG and secondary antibody did not show any fluorescent staining (fixed sperm: Fig. 2A—panels e, f; live sperm: Fig. 2B—panels e, f). Similarly, negative staining was obtained when SGG-preadsorbed anti-SGG IgG was used instead of anti-SGG IgG (data not shown). All of these results indicated that the fluorescent patterns observed in control and capacitated sperm were specific to SGG.

Capacitated sperm contained higher levels of DRMs enriched in SGG and cholesterol

Although lipid rafts have been isolated from mammalian sperm (Sleight et al., 2005; van Gestel et al., 2005; Shadan et al., 2004; Cross, 2004; Nishimura et al., 2001; Travis et al., 2001), their biochemical properties, especially their lipid profiles, have not been well characterized. Furthermore, since cholesterol efflux occurs as part of sperm capacitation (Flesch et al., 2001a; Visconti et al., 2002), it is important to determine whether this phenomenon affects the existence of lipid rafts in capacitated sperm. Fig. 3 shows that DRMs isolated from both control and capacitated sperm had similar properties to lipid rafts of somatic cells (Brown and London, 2000). Light scattering intensity (A_{400}) revealed that sperm DRMs were present in fractions #4, 5 and 6 around the interface between 5% and 30% sucrose in the ultracentrifuged tube of the Triton X-100 sperm lysate. In accordance with A_{400} values, the DRM fractions (#4, 5 and 6) contained higher cholesterol levels than the Triton X-100 soluble bottom fractions (#11, 12 and 13) (Fig. 3). The majority of proteins in the Triton X-100 sperm lysate was found in the bottom fractions. Since flotillin-2 exists selectively in lipid rafts of somatic cells and sperm (Rajendran et al., 2003; Cross, 2004), the sucrose gradient fractions were probed with anti-flotillin-2 antibody. In the control sperm sample, flotillin-2 (42 kDa) was present in DRM fractions #5, 6 as well as in the fractions #7 to 10. However, in capacitated sperm samples, flotillin-2 existed mainly in the DRM fractions (especially in fraction #5) (Fig. 3).

Significantly, the light scattering intensity (A_{400} value) of DRMs isolated from capacitated sperm was higher ($P < 0.001$) than that of DRMs from control sperm (Fig. 3 inset). This could reflect an increase in the aggregation of lipid raft units and/or in amounts of lipid rafts. The second possibility was supported by increased levels of the major lipid components, cholesterol + SGG + phospholipids, in capacitated sperm DRMs (0.64 μmoles in DRMs isolated from 1×10^9 sperm), compared with control sperm DRMs (0.35 μmoles in DRMs isolated from 1×10^9 sperm) (Fig. 4B). The amount of total proteins in capacitated sperm DRMs was also higher than in control sperm DRMs (108.88 ± 68.34 μg versus 49.93 ± 7.28 μg in DRMs isolated from 1×10^9 sperm). Notably, this increase in protein amount in capacitated sperm DRMs was proportional to the increase in the DRMs lipid content. Therefore, the proteins to lipids weight ratio of DRMs from both control and capacitated sperm was similar, i.e., 0.227 ± 0.017 and 0.255 ± 0.015.

Lipid quantification revealed that 20% of cholesterol in whole control sperm was present in their isolated DRMs. In capacitated sperm, 74% of cholesterol existed in their DRMs (Fig. 5). Similarly, a higher percentage of total SGG in sperm was present in capacitated sperm DRMs (71%), compared with control sperm DRMs (32%) (Fig. 5). The marked accumulation of cholesterol in capacitated DRMs was partly attributed to the lower level of cholesterol in whole sperm due to its efflux during capacitation (Fig. 4A). However, the levels of SGG and phospholipids were the same in control sperm and capacitated sperm (Fig. 4A). Therefore, the increase in SGG distribution in capacitated sperm DRMs directly reflected the enrichment of the sulfoglycolipid in these isolated membrane vesicles. Capacitated sperm also had a slight increase in proportion of phospholipids in DRMs compared with control sperm (i.e., 34% versus 20%) (Fig. 5). Although somatic cell DRMs are enriched in SM (Brown and Rose, 1992; Simons and Vaz, 2004), this enrichment was not observed in control sperm DRMs (22% in DRMs versus 20% in whole sperm). In capacitated sperm, the DRMs showed a slight increase in the SM content (36%), compared with the whole sperm (23%).

Although the level of DRMs increased in capacitated sperm, the ratio of the three main lipids, SGG/cholesterol/phospholipids, was similar in both capacitated and control sperm DRMs (1.0:2.0:3.4 versus 1.0:2.0:4.0) (Fig. 4B). These two ratios were, however, different from those lipid ratios in whole sperm, i.e., 1.0:3.3:6.8 for control sperm and 1.0:2.1:6.9 for capacitated sperm (Fig. 4A). This comparison indicated that the ratio of SGG to phospholipids was higher in DRMs than in whole sperm. This higher ratio of SGG to phospholipids in DRMs was indeed visually apparent by comparing HPTLC patterns of DRM lipids with whole sperm lipids (Fig. 4C). In this HPTLC, lipid samples of DRMs and whole sperm were loaded onto the plate based on an equal amount of SGG. Notably, the staining intensity of the three main phospholipids, PC, PE and SM, was lower in DRMs than in whole sperm, indicating the higher ratio of SGG to phospholipids in the isolated DRMs (Fig. 4C). The intensity ratio of PC to PE and SM in sperm DRMs appeared to be similar to that in corresponding whole sperm.

Phospholipids of lipid rafts isolated from somatic cells contain a higher degree of saturation, compared with total cellular phospholipids (Stulnig et al., 2001; Rouquette-Jazdanian et al., 2002). Since mammalian sperm uniquely contain high amounts of polyunsaturated PC and PE molecular species (with >40% of their fatty acyl chains being C22:6 and C22:5 (Parks and Lynch, 1992; Nikolopoulou et al., 1985)), the question of whether these PUFAs existed in PC and PE of the isolated sperm DRMs was addressed. FAME and DMA analyses of PC and PE in DRMs of both control sperm and capacitated sperm revealed that >85% of the hydrocarbon chains of both raft samples were saturated (mainly C16:0, with minor amounts of C18:0). Only 15% or less of these FAMEs + DMAs existed as C22:5.

Interaction of SGG with cholesterol

Since SGG possesses saturated hydrocarbon chains (Tanphaichitr et al., 2003), it was likely that SGG would interact with raft lipid components such as cholesterol. In fact, our unpublished FTIR spectroscopy results revealed that the hydrophobic interaction of cholesterol with DPPC and SGG resulted in a broadening of the phase transition curves of these lipid–cholesterol complexes, in accordance with previous findings on complexes of cholesterol with phospholipids and glycolipids (Ipsen et al., 1987; Ali et al., 1994; McMullen et al., 1996). Besides this hydrophobic interaction, the hydroxyl group of cholesterol may interact via hydrogen bonding with the ester carbonyl group of SGG and DPPC at the interfacial region of the bilayers. Our FTIR spectroscopy results supported this postulation for SGG. In the absence of cholesterol, the ester carbonyl stretching band of SGG displayed two distinct components at 1720 and 1740 cm^{-1}, reflecting the hydrogen-bonded and non-hydrogen bonded SGG molecular species, respectively (Fig. 6A, dash line). The apparent splitting of these two peaks is due to the crystal-like state of SGG bilayers, and thus minimal rotational movement of the ester carbonyl group (Attar et al., 2000). However, the relative intensity of the high frequency component of the ester carbonyl band of SGG diminished significantly, when the sulfoglycolipid existed with equimolar cholesterol in the binary liposomes. Concurrently, the intensity of the lower frequency (hydrogen-bonded) component increased (Fig. 6A, dash-dot line). These results indicated that the ester carbonyl group of SGG interacted via hydrogen bonding with the hydroxyl group of cholesterol (Fig. 6A). On the other hand, the ester carbonyl stretching band of DPPC was broad, representing two overlapping spectra of the non-hydrogen bonded and hydrogen bonded species; this is due to the ongoing rotational movement of the ester carbonyl group of DPPC. This DPPC ester carbonyl stretching band was not markedly affected by the presence of cholesterol (Fig. 6B, solid line and short dash line). This indicated that the ester carbonyl group of DPPC did not interact significantly with the hydroxyl group of cholesterol via hydrogen bonding. The ability of SGG to interact with cholesterol via both Van der Waal's force and hydrogen bonding suggested that SGG likely participated in formation of sperm DRMs.

Binding of pig sperm DRMs and APMs to homologous ZP

Mammalian sperm rafts have previously been shown to contain ZP-binding proteins (Nishimura et al., 2001; Sleight et al., 2005; van Gestel et al., 2005). SGG, a ZP adhesion molecule (White et al., 2000; Weerachatyanukul et al., 2001), was also present in pig sperm DRMs (Fig. 4). Therefore, it was pertinent to determine whether the isolated sperm DRMs could bind directly to homologous ZP and whether capaci-

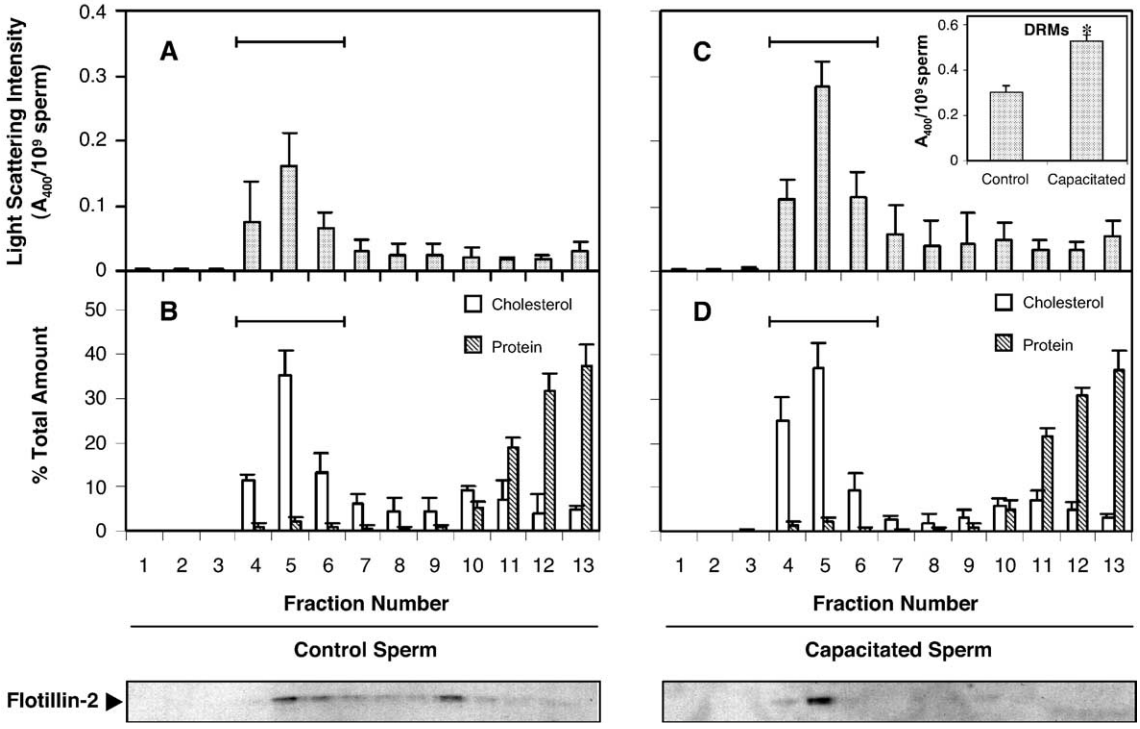

Fig. 3. Distribution of DRMs and their cholesterol and protein contents in the sucrose density gradient of sperm Triton X-100 lysate. The sperm lysate was prepared from an equal number (10^9 sperm) of control sperm (A, B) and capacitated sperm (C, D). Numbers in the *x* axis denote 1-ml fractions from top (#1) to bottom (#13) of the tube. Top panels (A, C) show light scattering intensity of each fraction. Note that DRMs banded at fractions #4, 5 and 6 (cropped bar). Bottom panels (B, D) show percent cholesterol and total proteins in each fraction, with their total amounts in the tube being 100%. Results were expressed as means ± SD's of the mean values from 3 experiments carried out on different days. An equal volume of each fraction was probed for a raft marker, flotillin-2, by immunoblotting; results shown are representative of 2 replicate experiments. Inset: sums of A_{400} values of fractions 4 to 6 (DRMs) of control and capacitated sperm. * Denotes significant difference of A_{400} values between the two sperm DRMs samples.

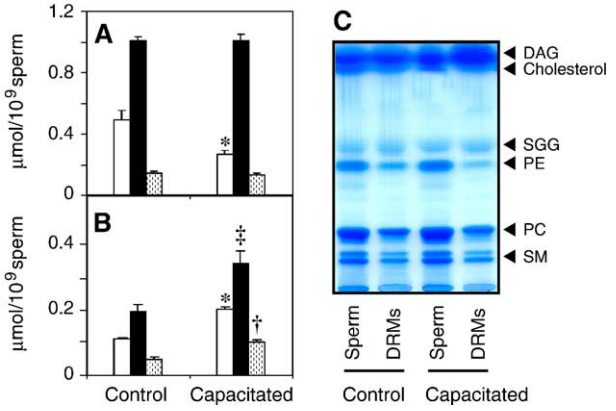

Fig. 4. Lipid composition of whole sperm and isolated DRMs. Levels of cholesterol (white bar), total phospholipids (black bar) and SGG (dashed bar) were shown for 1×10^9 whole sperm (both control and capacitated) (A), and DRMs isolated from the same number of the two sperm types (B). Data were expressed as means ± SD's of the mean values from 3 different sperm and DRMs samples. (C) HPTLC lipid profiles of whole sperm and isolated DRMs. All samples were spotted onto the HPTLC plate based on an equal amount (3 μg) of SGG. DAG=diacylglycerol. HPTLC results shown are representative of two sets of sperm and DRMs samples. *, ‡, † Each denotes significant difference of the corresponding lipid values between capacitated and control sperm samples.

tated sperm DRMs had greater ZP binding ability than control sperm DRMs. DRMs isolated from both control sperm (Fig. 7A, ○–○) and capacitated sperm (Fig. 7A, □–□) had an affinity for solubilized Alexa-430 ZP. The fluorescence intensity of DRM-bound Alexa-430 ZP increased and approached saturation with increasing concentrations of free Alexa-430 ZP. The levels of non-specific binding of Alexa-430 ZP to control and capacitated sperm DRMs also rose with increasing amounts of free Alexa-430 ZP (0–0.4 μM), but in a linear manner, and the levels were only 0–25% of the total levels of the DRMs-bound Alexa-430 ZP (Fig. 7A, dashed lines). Curves of specific binding of Alexa-430 ZP to control sperm DRMs and capacitated sperm DRMs (obtained by subtracting the non-specific binding from the total binding of Alexa-430 ZP) revealed that capacitated sperm DRMs had a significantly higher affinity and greater capacity to interact with Alexa-430 ZP ($P < 0.05$) (Fig. 7B). K_d values of Alexa-430 ZP-sperm DRMs binding were 0.056 ± 0.02 μM and 0.11 ± 0.03 μM for capacitated and control sperm, respectively. This indicated a higher affinity of capacitated sperm DRMs for ZP, compared with control sperm DRMs. Notably, K_d of the binding of APMs, isolated from capacitated sperm, to Alexa-430 ZP was similar to that of capacitated sperm DRMs–ZP binding, i.e., 0.058 ± 0.01 μM. The maximum ZP binding capacity (B_{max}) of capacitated sperm DRMs was also higher than that of control sperm DRMs (i.e., 0.250 ± 0.006 pmol/0.5 μg DRM proteins versus 0.186 ± 0.002 pmol/0.5 μg DRM protein). In contrast, both control sperm DRMs and capacitated sperm DRMs showed a minimum affinity for Alexa-430 ovalbumin (Fig. 7A, △–△). When DRMs isolated from sperm tails were used for incubation with Alexa-430 ZP in place of DRMs prepared from whole sperm, the levels of Alexa-430 ZP binding to sperm tail DRMs were similar to the non-specific binding of Alexa-430 ZP to whole sperm DRMs (Fig. 7A, ▽–▽). This suggested that the binding of Alexa-430 ZP to the tail DRMs was also non-specific.

Pig ZP(B + C), a hetero-oligomer of ZPB and ZPC glycoproteins, has previously been shown to be a pig sperm receptor. In competitive sperm APMs–ZP binding assays, using purified ZP(B + C), as well as purified ZPB and ZPC (both slightly deglycosylated), Yurewicz et al. (1993, 1998) have shown that ZPB is a major participant in pig sperm–ZP binding, although the co-existence of ZPC is also essential for this interaction. If sperm DRMs represent the ZP-binding domains on sperm, the binding of sperm rafts to ZP would then be dependent on pig ZP(B + C), and would be effectively competed by purified ZPB. Results from our competitive sperm DRMs-Alexa-430 ZP binding assays supported this postulation. Purified pig ZP(B + C) (Fig. 8A, ▼–▼) competitively inhibited the binding of Alexa-430 ZP to capacitated pig sperm DRMs to the same extent as solubilized whole pig ZP (Fig. 8A, ▲–▲). At 4 μM of solubilized ZP or ZP(B + C), inhibition was at the maximum (Fig. 8A). When purified ZPB or ZPC in the same concentration range as ZP(B + C) was included as a competitor ZP ligand in the sperm DRM-Alexa-430 ZP co-incubates, ZPB exhibited a greater inhibitory effect on sperm DRMs-Alexa-430 ZP binding than ZPC (80% maximum inhibition versus 30%) (Fig. 8B). These results suggested that the interaction between sperm DRMs and ZP was dependent on pig ZP(B + C), a result similar to that observed for sperm APMs–ZP interaction (Yurewicz et al., 1998). The result on the higher ability of purified ZPB to compete with sperm DRMs–ZP binding was also similar to the results obtained in competitive sperm APMs–ZP binding experiments (Yurewicz et al., 1993, 1998), and this further suggested the importance of ZPB in pig sperm–ZP binding. However, the lower ability of purified ZPC (orthologous to mouse ZP3, the primary mouse sperm receptor, Wassarman, 2005) to inhibit the binding between pig ZP and sperm DRMs (Fig. 8) and sperm APMs (Yurewicz et al., 1993) may still be argued to be attributed to its partial deglyco-

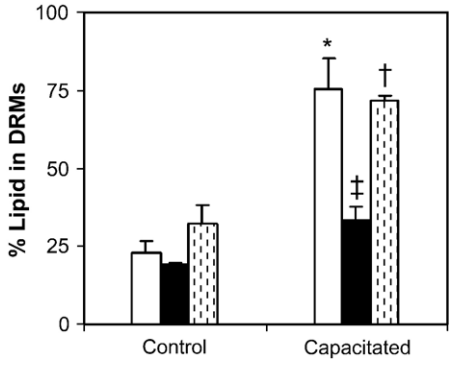

Fig. 5. Distribution of sperm cholesterol, phospholipids and SGG in DRMs. Percentages of cholesterol (white bar), total phospholipids (black bar), and SGG (dashed bar) in sperm that were present in control and capacitated sperm DRMs are shown. These percentages were calculated from the data shown in Figs. 4A and B and were expressed as means ± SD's of the values obtained from the 3 sets of experiments. *, ‡, † Each denotes significant difference of the corresponding lipid values between the capacitated sample and the control sample.

sylation required for its purification. Since glycosylated moieties of pig ZP are important for sperm–ZP binding (Yurewicz et al., 1993), we also determined their involvement in the binding of sperm DRMs to solubilized ZP. Deglycosylated ZP had a much less inhibitory effect on sperm DRMs–ZP binding than the solubilized whole ZP (Fig. 8A, +–+). At 4 μM, deglycosylated ZP induced only 40% inhibition, compared with >90% by whole ZP glycoproteins (Fig. 8A). This indicated the significance of ZP carbohydrate moieties in sperm DRMs–ZP binding. In contrast, 0–4 μM ovalbumin showed <20% inhibition of sperm DRMs–ZP binding (Fig. 8A, ×–×). All of these results indicated that the mechanisms of sperm DRMs binding to the ZP were similar to those of sperm–ZP binding (Yurewicz et al., 1993, 1998).

Participation of SGG in sperm DRMs–ZP binding

We have previously demonstrated that SGG, a sperm DRM component (Fig. 4), had a direct affinity for ZP (White et al., 2000; Weerachatyanukul et al., 2001). Therefore, it was likely that the binding of sperm DRMs to the ZP was dependent on SGG. This hypothesis was supported by results in Fig. 9A. Pretreatment of capacitated sperm DRMs with affinity purified anti-SGG IgG (Fig. 9A) or anti-SGG Fab (Fig. 9B) decreased the binding of DRMs to the ZP dose-dependently. In contrast, pretreatment of sperm DRMs with preimmune rabbit serum IgG did not result in inhibition of sperm DRMs–ZP binding. Notably, the maximum inhibition of sperm DRMs–ZP binding occurred at a concentration of the monovalent anti-SGG Fab (i.e., 7.2 μM) and bivalent anti-SGG IgG (i.e., 3.6 μM) that gave the same number of antigen-binding domains. Therefore, the inhibitory effects of anti-SGG IgG were not likely due to steric hindrance. However, the maximum inhibition of sperm DRMs–ZP binding induced by anti-SGG Fab was lower than that observed with anti-SGG IgG (60% versus 85%) (Figs. 9A, B). This may be due to steric hindrance of anti-SGG IgG on molecules adjacent to SGG on the sperm surface.

Binding of Alexa-430 ZP to SGG containing liposomes was also investigated. The constructed liposomes contained SGG, cholesterol and DPPC with the same molar ratio as that of these lipid classes in capacitated sperm DRMs (i.e., 1.0:2.0:3.4). DPPC was used as the model phospholipid, since the majority of the fatty acyl chains in PC and PE of sperm DRMs was C16:0. Fig. 9C shows that SGG containing liposomes interacted with Alexa-430 ZP. The fluorescence intensity of Alexa-430 ZP that bound to SGG containing liposomes increased and approached saturation with increasing concentrations of free Alexa-430 ZP (Fig. 9C). Although non-specific binding of Alexa-430 ZP to SGG containing liposomes (measured in the presence of excess unlabeled ZP) increased linearly (Fig. 9C, ▼–▼), its levels were only 0–25% of that observed for the total levels of Alexa-430 ZP binding to SGG containing liposomes (Fig. 9C, ○–○). Subtraction of this non-specific binding from the total binding of Alexa-430 ZP to SGG containing liposomes yielded the specific binding curve (Fig. 9C, ●–●) with a K_d value of 0.085 ± 0.032 μM for the interaction between Alexa-430 ZP and SGG containing liposomes. In contrast, SGG-depleted liposomes, containing cholesterol and DPPC, interacted with Alexa-430 ZP at much lower levels (0–35% of the total levels of Alexa-430 ZP binding to SGG containing liposomes) (Fig. 9C, △–△), and this interaction increased linearly, a pattern typical of non-specific binding of Alexa-430 ZP to SGG containing liposomes. All of these results strongly suggested that Alexa-430 ZP bound specifically to SGG in the SGG containing liposomes.

Discussion

Sperm DRMs were used to validate our hypothesis that sperm lipid rafts have ZP binding ability. We chose to use Triton X-100 as the non-ionic detergent in the preparation of sperm DRMs for a few reasons. First, Triton X-100 has been widely used for DRMs preparation in somatic and gamete cells (Brown and Rose, 1992; Schuck et al., 2003; Shogomori and Brown, 2003; Pike, 2004; Cross, 2004; Shadan et al., 2004;

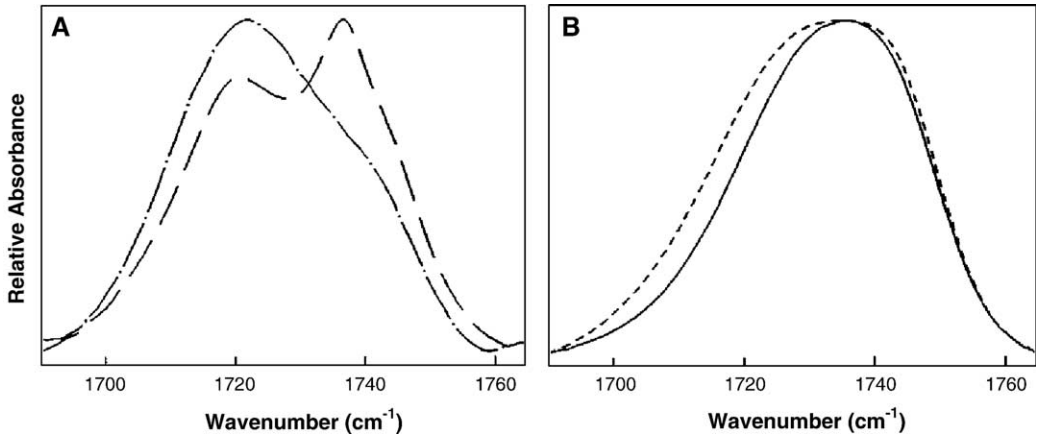

Fig. 6. Intermolecular hydrogen bonding between SGG and cholesterol as detected by FTIR spectroscopy. (A) Ester carbonyl stretching band of SGG (long dash), and an equimolar mixture of SGG-cholesterol (dot-long dash). (B) Ester carbonyl stretching band of DPPC (solid line), and an equimolar mixture of DPPC-cholesterol (small dash). Results shown are representative of three experiments performed on different days.

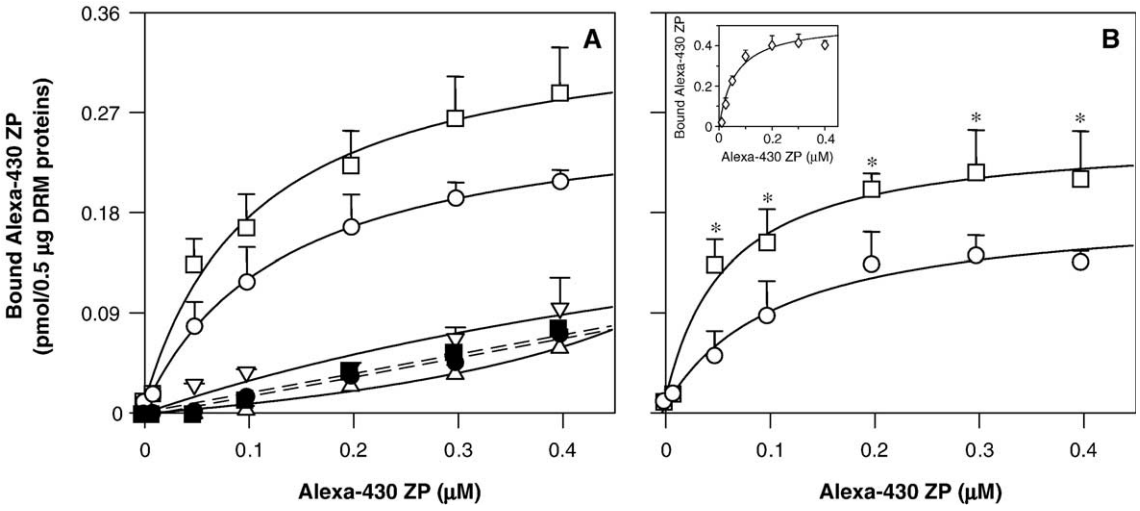

Fig. 7. Binding of pig sperm DRMs and APMs to homologous ZP. (A) Alexa-430 ZP binding to DRMs isolated from control sperm (○), capacitated sperm (□), and sperm tails (▽). Non-specific binding of control sperm DRMs (●) and capacitated sperm DRMs (■) to Alexa-430 ZP is shown as dashed lines. Low levels of interaction between capacitated sperm DRMs (△) with Alexa-430 ovalbumin, an inert protein were observed. The *y* axis represents the levels of Alexa-430 ZP bound to sperm DRMs, except for the Alexa-430 ovalbumin experiment in which the axis denotes the levels of the bound Alexa-430 ovalbumin. (B) Specific binding of Alexa-430 ZP to control sperm DRMs (○) and capacitated sperm DRMs (□), obtained by subtracting non-specific binding levels from total binding levels of Alexa-430 ZP (shown in panel A). Inset: Alexa-430 ZP binding to APMs isolated from capacitated sperm. Data shown were specific binding (i.e., already corrected for the non-specific binding, which was ~10% at the highest Alexa-430 ZP concentration). Data expressed are means ± SD's of the mean values from 3 experiments performed on different days except for the experiments that determined the non-specific binding of Alexa-430 ZP to sperm DRMs (A), which were done twice, and the representative data from one experiment are shown. * Denotes significant differences in the levels of ZP binding between control and capacitated sperm DRMs.

Maehashi et al., 2003; Ohta et al., 1999) and its mechanisms in generating DRMs have been more studied than other non-ionic detergents (Shogomori and Brown, 2003; London and Brown, 2000). Using a series of non-ionic detergents to treat MDCK and Jurkat T cells, Schuck et al. (2003) have shown that Triton X-100 (when used at a low ratio to cellular proteins, and at low temperatures) is more selective for yielding DRMs that contain known components of lipid rafts (e.g., cholesterol, sphingolipids, saturated phospholipids, caveolin-1). Therefore, Simons and colleagues have suggested the use of Triton X-100 as the first detergent to isolate low-density DRMs (Schuck et al., 2003). Nonetheless, Panasiewicz et al. (2003) have pointed out that the low weight ratio of Triton X-100 to cellular proteins is of crucial importance to obtain an optimum yield of low-density DRMs. Results from our pilot studies indicated that the weight ratio of 0.2 of Triton X-100 to cellular proteins consistently gave the highest yield of low density DRMs from both control and capacitated pig sperm, and therefore, this ratio was used in the DRMs isolation described herein.

DRMs isolated from pig sperm had a number of unique properties. First, the male germ cell-specific sulfoglycolipid, SGG, was a component of sperm DRMs. This result corroborates previous findings that SGC (SGG analog) is present in DRMs of sea urchin sperm and MDCK cells (Ohta et al., 1999; Brown and Rose, 1992). Capacitated sperm DRMs, in particular, were enriched in both SGG and cholesterol. In

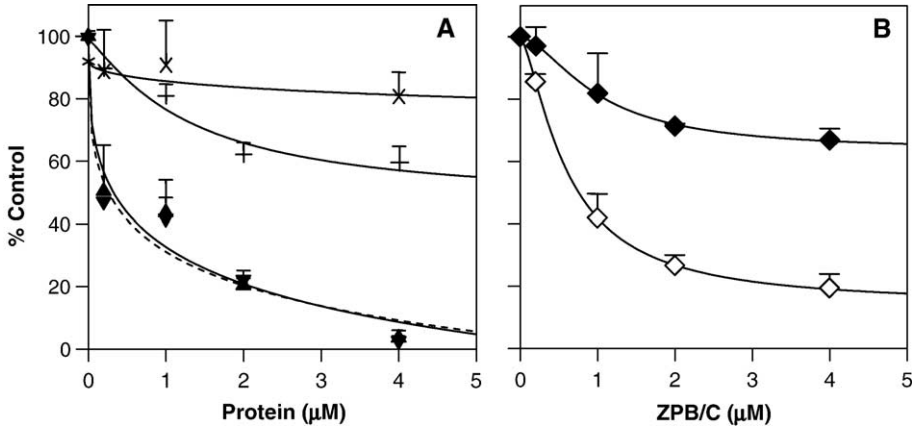

Fig. 8. Involvement of ZP glycoproteins and their carbohydrate moieties in sperm DRMs–ZP binding. Capacitated sperm DRMs were incubated with 0.2 µM Alexa-430 ZP in the presence of 0 to 4 µM of solubilized whole pig ZP (▲), ZP(B + C) glycoproteins (▼),TFMS-deglycosylated ZP (+), or ovalbumin (×) (A); and with ZPB (◊) and ZPC (⧫) (B). The levels of Alexa-430 ZP bound to capacitated sperm DRMs in the presence of these ligands were expressed as percentages of the values obtained from the sperm DRMs-Alexa-430 ZP co-incubates that contained no competitor ligands. Data are expressed as means ± SD's of the mean values of 3 experiments performed on different days.

contrast to results observed in somatic cells (Brown and Rose, 1992; Schuck et al., 2003), sperm DRMs were not enriched in SM (Fig. 4). The existence of SGG in sperm DRMs was likely due to its ability to interact hydrophobically with cholesterol, a pertinent DRMs component, as well as with saturated phospholipids (Tanphaichitr et al., 2003; Attar et al., 2000), which we also showed to be present in sperm DRMs. We further showed that hydrogen bonding was another interaction mode between SGG and cholesterol, a prominent feature of SGG, since DPPC (having 16:0/16:0 hydrocarbon chains like SGG) did not exhibit significant hydrogen bonding with cholesterol (Fig. 6). The propensity of SGG to form hydrogen bonds with cholesterol was perhaps due to restricted rotational movement of its ester carbonyl group (Attar et al., 2000); thus the hydrogen bonds, once formed, were retained. The tight interaction between SGG and cholesterol corroborated our unpublished results showing that the SGG–cholesterol liposomes were insoluble in 1% Triton X-100 when cholesterol content was higher than 30 mol%. In contrast, SGG liposomes were completely soluble in this detergent.

Sperm capacitated in CM containing bicarbonate and BSA showed a significant decrease in the levels of cholesterol, but not phospholipids or SGG (Fig. 4). Bicarbonate first induces modification of the lipid architecture via phospholipid scrambling, and subsequently BSA induces a release of cholesterol from sperm (Flesch et al., 2001a). It is tempting to speculate that cholesterol is released from the non-raft microdomains during capacitation, although this postulation still needs experimental validation. Cholesterol efflux would lead to a global increase in membrane fluidity in capacitated sperm (Wolf et al., 1986). Changes of the SGG localization patterns in capacitated sperm, compared with control sperm (Fig. 2), were one line of evidence supporting this membrane remodeling hypothesis during capacitation. This remodeling would allow SGG, cholesterol and saturated phospholipid molecules, present in the non-raft areas, to regroup themselves via their inherent affinity for each other (i.e., hydrophobic interactions and hydrogen bonding). As a result, new stretches of the lipid rafts would form, and

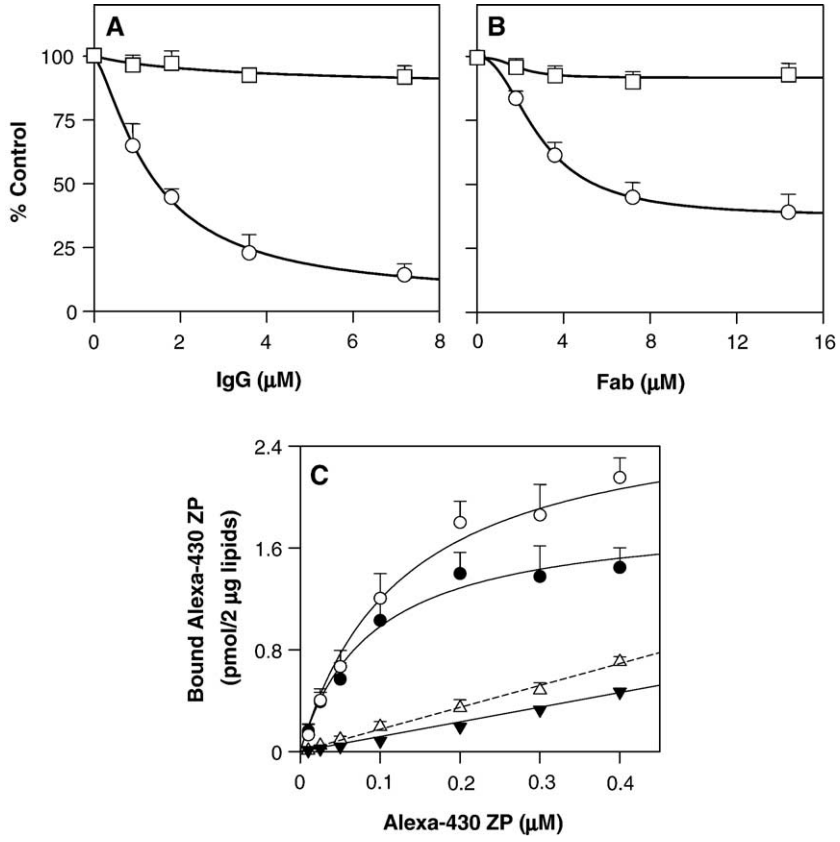

Fig. 9. Participation of SGG in DRMs–Alexa-430 ZP binding. (A and B): Capacitated sperm DRMs were treated with anti-SGG IgG (A) or Fab (B) (○) or with preimmune rabbit serum IgG (A) or Fab (B) (□) prior to co-incubation with Alexa-430 ZP. The levels of Alexa-430 ZP bound to antibody-treated sperm DRMs are expressed as percentages of the values obtained from the untreated sperm DRMs–Alexa-430 ZP co-incubates. Data shown in panels A and B were pooled from two experiments performed on different days. For each day, 3 replicates of each DRMs sample were used for treatment with each antibody concentration; data from the six points for each antibody concentration, showing less than 10% variation, were then calculated for means ± SD's. (C) SGG–cholesterol–DPPC liposomes (molar ratio: 1.0:2.0:3.4) exhibited affinity for Alexa-430 ZP. The SGG-containing liposomes were incubated with various concentrations of Alexa-430 ZP, and the fluorescence intensity of liposomes-bound Alexa-430 ZP was measured (○). (▼) Non-specific binding of Alexa-430 ZP to SGG-containing liposomes. (●) Specific binding of Alexa-430 ZP to SGG-containing liposomes, obtained by subtracting the non-specific binding values from the total binding levels of Alexa-430 ZP to the SGG-containing liposomes. (△) Binding levels of Alexa-430 ZP to SGG-depleted (cholesterol–DPPC, molar ratio, 2.0:3.4) liposomes. All liposome–Alexa-430–ZP binding assays were done 3 times on different days and data are expressed as means ± SD's of the values obtained from the 3 experiments. However, the assay for non-specific binding of Alexa-430 ZP to SGG-containing liposomes was done twice, and the data shown are averaged values from the two experiments.

these microdomains may coalesce or aggregate with preexisting lipid rafts in the sperm membrane (Fig. 10A). This would result in higher levels of DRMs extracted from capacitated sperm (Fig. 3). The aggregation of lipid rafts may induce sperm signaling events (Simons and Ehehalt, 2002; Harder, 2004). The non-raft microdomains would then be left with a higher proportion of unsaturated phospholipids, which would endow higher fluidity to these areas (Fig. 10A). This may be beneficial to fusion events during the acrosome reaction (Primakoff and Myles, 2002). Significantly, data presented here argue that cholesterol efflux, occurring as part of capacitation, did not compromise sperm lipid raft formation. Our results corroborated previous observations in pig sperm "capacitated" by treatment with cyclodextrin (Shadan et al., 2004). In addition, in TRVb-1 cells (modified Chinese hamster ovary cells), cholesterol depletion leads to formation of larger ordered membrane microdomains (Hao et al., 2001). However, contradicting results were described in mouse sperm (Sleight et al., 2005). The authors did not visualize the DRMs band on the sucrose gradient of the Triton X-100 lysate of capacitated mouse sperm, following ultracentrifugation. Notably, the weight ratio of Triton X-100 to sperm proteins used in this study was much higher than that used by us and Shadan et al. (2004) (i.e., 0.6 versus 0.2). This may have led to destruction or weakening of the interaction between cholesterol and saturated lipids in the liquid-ordered microdomains. Supporting this idea, our unpublished work indicates that DRMs exist in capacitated mouse sperm, when the weight ratio of Triton X-100 to sperm proteins is kept at 0.2.

While lipid rafts are implicated as platforms for cell adhesion and signaling molecules (Simons and Ehehalt, 2002; Brown and London, 2000; Hakomori, 2000; Horejsi, 2003), evidence revealing direct involvement of isolated lipid rafts in cell adhesion is still limited (Maehashi et al., 2003; Iwabuchi et al., 2000). In this report, we showed for the first time that pig sperm DRMs possessed an ability to bind to solubilized ZP in a specific manner based on the following results. First, the levels of Alexa-430 ZP binding to sperm DRMs approached saturation at increasing concentrations of Alexa-430 ZP. Second, the binding of Alexa-430 ZP to sperm DRMs could be effectively competed with an excess amount of non-fluorescently labeled solubilized ZP. Third, sperm DRMs exhibited only background binding levels to Alexa-430 ovalbumin (known for its inability to bind to sperm, Carmona et al., 2002b) (Fig. 7). Although sperm DRMs used in this binding assay were mixtures of lipid rafts from whole sperm, the sperm DRMs responsible for this ZP binding were likely from the sperm head, the site of ZP binding, since DRMs isolated from sperm tails exhibited background binding to ZP glycoproteins (Fig. 7A). This postulation was supported by the observation that the K_d value of capacitated pig sperm DRMs-ZP binding (0.056 μM) was similar to that of capacitated pig sperm APMs-ZP binding (0.058 μM, Fig. 7B) and also to that of capacitated mouse sperm-ZP binding (0.067 μM, Kerr et al., 2002). However, the lower B_{max} value of sperm DRMs-ZP binding (0.25 pmol ZP/0.5 μg protein), compared with sperm APMs-ZP binding (0.52 pmol ZP/0.5 μg protein), suggested that the ZP binding molecules in DRMs of the sperm anterior head plasma membrane were diluted with other DRM molecules belonging to the sperm tail and other parts of sperm. Most importantly, the mechanisms of sperm DRMs-ZP binding appeared to be the same as those utilized in sperm–ZP interaction. This was evidenced by the observations that ZP(B + C), the heterodimer of ZPB and ZPC glycoproteins that is the sperm receptor (Yurewicz et al., 1993, 1998), could competitively inhibit capacitated sperm DRMs–ZP binding to a minimum level, similar to solubilized whole ZP (Fig. 8). In previous comparisons, using slightly deglycosylated ZPB and ZPC, ZPB was more effective in inhibiting sperm APMs–ZP binding (Yurewicz et al., 1993, 1998). Our results indicated a similar efficiency of ZPB in competitively inhibiting sperm DRMs–ZP binding more efficiently than ZPC. The significance of carbohydrate moieties of ZP glycoproteins in sperm–ZP interaction was also evidenced in sperm DRMs–ZP binding, since deglycosylated ZP polypeptides exhibited minimal inhibition of this binding event (Fig. 8). All of these results strongly suggest that lipid raft microdomains may be the ZP interaction sites on the sperm membranes. The greater ZP binding ability of capacitated sperm may thus be explained by the higher ZP affinity (higher B_{max} and lower K_d) of their DRMs, compared with that of control sperm DRMs (Fig. 7), and possibly the higher amounts of exposed lipid raft microdomains (Figs. 3 and 4). Since the major lipid components of DRMs from both capacitated and control sperm were the same (Fig. 4), the lower K_d value of capacitated sperm DRMs for ZP binding, compared with control sperm DRMs, may be due to the presence of additional proteins with higher affinity for the ZP in the former. On the other hand, the higher B_{max} observed for capacitated sperm DRMs in ZP binding would likely reflect the increased quantity of ZP binding proteins in these DRMs. It is also possible that clustering of ZP binding molecules in capacitated sperm DRMs may enhance their ZP affinity (lower K_d) through their cooperative action in ZP binding. Arylsulfatase A (AS-A—a ZP binding component of SLIP1, a conglomerate of SGG binding proteins (Tanphaichitr et al., 1998)) may be one of these sperm surface protein candidates, since AS-A has affinity for both SGG (one of the major lipid component of sperm DRMs) and the ZP (Tanphaichitr et al., 2003), and its interaction with the ZP is highly dependent on ZPB (Carmona et al., 2002a), a property similar to the binding between sperm DRMs and ZP. In fact, our unpublished results reveal a higher amount of AS-A in the DRMs isolated from capacitated sperm, compared with DRMs prepared from control sperm. Together, with a global increase in membrane fluidity in capacitated sperm due to cholesterol efflux, DRMs on these sperm, upon ZP binding, would have a greater tendency to cluster to form macrorafts; sperm signaling events may then occur (Simons and Ehehalt, 2002; Harder, 2004). Studies are underway in our laboratory

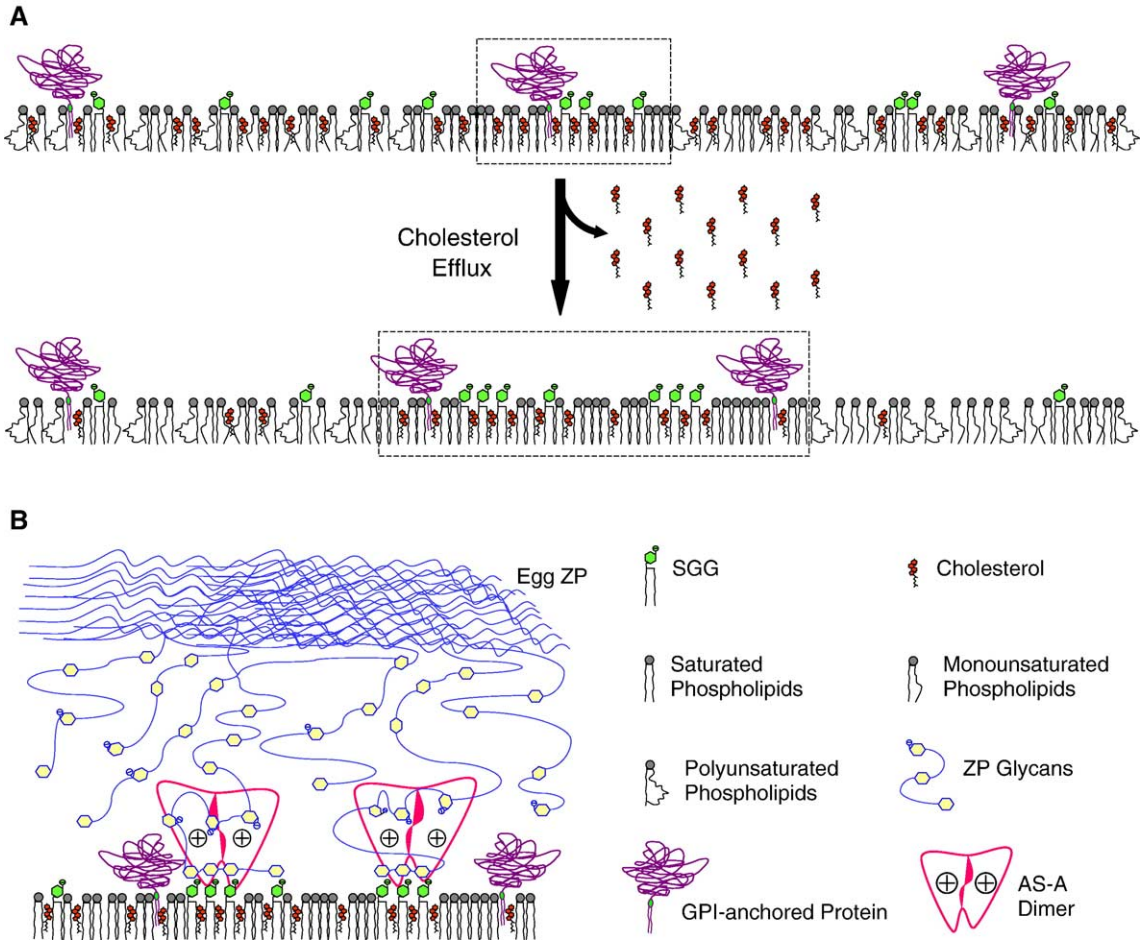

Fig. 10. (A) Hypothetical models for an increase in lipid rafts microdomains in the sperm plasma membrane following capacitation. For simplicity, only the outer plasma membrane leaflet is shown in this model as well as in the model in panel B. In control sperm, ~30% of SGG was in the lipid rafts (cropped in a dashed-line square). These SGG molecules interact with cholesterol and saturated phospholipids. Some GPI-linked proteins may also exist in control sperm lipid rafts via the interaction of their acyl chains with the saturated fatty acyl chains of phospholipids. The remaining SGG molecules are in the non-raft areas, which contain a high percentage of phospholipids with one of their acyl chains being mono- or polyunsaturated. However, the other acyl chain of these phospholipids is mainly saturated, thus interacting with the hydrocarbon chains of SGG in the non-raft areas. Cholesterol also coexists with SGG and phospholipids in the fluid non-raft areas, interacting with their saturated hydrocarbon chains or monounsaturated acyl chains with the double bond deep below the membrane interface. During capacitation, cholesterol is likely to be released from the non-raft areas, resulting in a further increase in fluidity. Scramblase is also activated allowing lipids to reorganize themselves (Flesch et al., 2001a). SGG, cholesterol and saturated phospholipids would regroup together, thus forming new patches of lipid rafts, which may coalesce with preexisting lipid raft microdomains in the sperm plasma membrane. (B) Hypothetical model of how SGG molecules in sperm lipid rafts interact with the ZP glycans. The ZP glycans likely interact with the galactosyl sulfate moiety of SGG. However, since this monosaccharide head group would rise only a short distance above the sperm membrane layer, it would be difficult for the ZP glycans to reach this head group without additional anchoring force. AS-A, a peripheral plasma membrane protein which exists in a dimeric form at physiological pH, has affinity for both SGG and the ZP (Carmona et al., 2002a,b). AS-A may first bind to the ZP glycans (possibly via interaction between positively charged amino acids of AS-A and sulfated sugar residues of the glycans) and attract them to the sperm plasma membrane for the interaction with the galactosyl sulfate lawn of SGG molecules. Although the carbohydrate–carbohydrate interactions between the galactosyl sulfate groups of SGG and ZP glycans are not strong, they may be stabilized by the multiplicity of SGG molecules in the lipid raft microdomains.

to determine whether sperm DRMs contain ZP-binding molecules and signaling molecules, and whether these molecules colocalize on the live capacitated sperm surface.

We have demonstrated previously that SGG is involved in sperm–ZP binding, and that SGG is localized specifically on the sperm head surface, the site of ZP interaction in mice and humans (White et al., 2000; Weerachatyanukul et al., 2001). Indirect immunofluorescence of SGG in pig sperm confirms its exclusive localization at the ZP binding site, the sperm head. Confocal microscopy also indicated globular SGG patterns. Since the globular units of immunostained SGG were present in both fixed and live sperm (Fig. 2), they were unlikely to result from capping and patching phenomena induced by bivalent antibodies (Harder and Simons, 1999). These globular patterns likely reflected clusters of SGG molecules due to their propensity to interact among themselves (Attar et al., 2000; Tanphaichitr et al., 2003) as well as with cholesterol and/or other proteins, such as AS-A (Carmona et al., 2002a,b; Tanphaichitr et al., 2003). Notably, indirect immunofluorescence of SGC, a SGG analog, on the plasma membrane of aldehyde fixed renal distal tubule epithelial cells also reveals punctate staining patterns (Saravanan et al., 2004). Globular fluorescent staining patterns have also been observed with another

acidic glycolipid, GM1, as detected by chlolera toxin in aldehyde fixed fibroblasts (Palazzo et al., 2004). Clustering of these glycolipids is likely due to Van der Waal's interaction between their hydrocarbon chains as well as intermolecular hydrogen bonding that involves the hydroxyl groups of the glycolipid's sugar moiety (Hakomori, 2000; Simons and Vaz, 2004).

Possessing ZP affinity, SGG molecules in sperm DRMs would likely contribute to the ZP binding ability of sperm DRMs. Results in Fig. 9 verified this postulation. In fact, the K_d (0.085 μM) of the binding between ZP and SGG containing liposomes (having the same lipid constituents as sperm DRMs) was in the same range as that of sperm DRMs–ZP binding (0.052 μM and 0.110 μM for capacitated and control sperm DRMs, respectively), indicating the significance of the SGG-containing membrane areas in DRMs in this binding event. Presumably, it is the galactosyl sulfate head group of SGG that is directly involved in ZP binding. However, since this monosaccharide head group would only rise a short distance above the lipid bilayer, the interaction of SGG molecules with the ZP glycoproteins may be subsequent to the initial interaction between the ZP glycans and ZP-binding proteins that protrude high above the sperm plasma membrane bilayers. AS-A, which is a peripheral plasma membrane protein with affinity for both SGG and ZP glycans (Carmona et al., 2002a,b), would be an ideal candidate for this initial sperm–ZP interaction. As shown in our hypothetical model (Fig. 10B), AS-A would first interact with the ZP glycans, perhaps via its affinity for ZP sulfated sugars. This binding would draw the ZP glycans next to the surface of the sperm lipid rafts, thus allowing carbohydrate–carbohydate interaction between the ZP saccharide chains and the galactosyl sulfate group of SGG. Although this type of interaction is not strong, it can be stabilized by the "Velcro" mechanism due to the multiplicity of SGG molecules in the lipid rafts. The postulated dependence of other sperm DRM component(s) in the involvement of SGG in sperm DRMs–ZP binding was supported by our results showing only 60% maximum inhibition of sperm DRMs–ZP binding when the DRMs were pre-incubated with anti-SGG Fab. The SGG–ZP interaction may in turn further support the initial binding of AS-A to the ZP. The mechanism of the involvement of SGG in sperm lipid rafts-ZP binding may be common to all mammalian sperm, since SGG is a conserved molecule (Tanphaichitr et al., 2003). Identities of other ZP binding proteins that co-exist with SGG in the sperm lipid rafts would bring about a clearer understanding of the involvement of SGG in sperm lipid rafts–ZP interaction, and proteomic analyses of capacitated sperm DRMs are ongoing in our laboratory. Nonetheless, our results on SGG support the concept that glycolipids are significant in cell adhesion/signaling via their contribution to formation and functions of lipid rafts (Hakomori, 2000; Harder and Simons, 1999; Maehashi et al., 2003).

Acknowledgments

This work was funded by CIHR and NSERC (to NT), an Ontario Graduate Scholarship (to MB), STIRRHS fellowships (to KC and HX), and a Thailand Research Fund fellowship (to WW). Assistance of T. van Gulik in manuscript preparation is acknowledged.

References

Ali, S., Smaby, J.M., Brockman, H.L., Brown, R.E., 1994. Cholesterol's interfacial interactions with galactosylceramides. Biochemistry 33, 2900–2906.

Attar, M., Kates, M., Bou Khalil, M., Carrier, D., Wong, P.T.T., Tanphaichitr, N., 2000. A Fourier-transform infrared study of the interaction between germ-cell specific sulfogalactosylglycerolipid and dimyristoylglycerophosphocholine. Chem. Phys. Lipids 106, 101–114.

Baltz, J.M., Katz, D.F., Cone, R.A., 1988. Mechanics of sperm–egg interaction at the zona pellucida. Biophys. J. 54, 643–654.

Bou Khalil, M., Carrier, D., Wong, P.T.T., Tanphaichitr, N., 2001. Polymorphic phases of galactocerebrosides: spectroscopic evidence of lamellar crystalline structures. Biochim. Biophys. Acta 1512, 158–170.

Brown, D.A., London, E., 2000. Structure and function of sphingolipid- and cholesterol-rich membrane rafts. J. Biol. Chem. 275, 17221–17224.

Brown, D.A., Rose, J.K., 1992. Sorting of GPI-anchored proteins to glycolipid-enriched membrane subdomains during transport to the apical cell surface. Cell 68, 533–544.

Burkin, H.R., Miller, D.J., 2000. Zona pellucida protein binding ability of porcine sperm during epididymal maturation and the acrosome reaction. Dev. Biol. 222, 99–109.

Carmona, E., Weerachatyanukul, W., Soboloff, T., Fluharty, J.L., White, D., Promdee, L., Ekker, M., Berger, T., Buhr, M., Tanphaichitr, N., 2002a. Arylsulfatase A is present on the pig sperm surface and is involved in sperm–zona pellucida binding. Dev. Biol. 247, 182–196.

Carmona, E., Weerachatyanukul, W., Xu, H., Fluharty, A., Anupriwan, A., Shoushtarian, A., Chakrabandhu, A., Tanphaichitr, N., 2002b. Binding of arylsulfatase A to mouse sperm inhibits gamete interaction and induces the acrosome reaction. Biol. Reprod. 66, 1820–1827.

Cross, N.L., 2004. Reorganization of lipid rafts during capacitation of human sperm. Biol. Reprod. 71, 1367–1373.

Duck-Chong, C.G., 1979. A rapid sensitive method for determining phospholipid phosphorus involving digestion with magnesium nitrate. Lipids 14, 492–497.

Flesch, L.J., Colenbrander, B., van Golde, L.M., Gazella, L.M., 1999. Capacitation induces tyrosine phosphorylation of proteins in the boar sperm plasma membrane. Biochem. Biophys. Res. Commun. 262, 787–792.

Flesch, F.M., Brouwers, J.F., Nievelstein, P.F., Verkleij, A.J., Van Golde, L.M., Colenbrander, B., Gadella, B.M., 2001a. Bicarbonate stimulated phospholipid scrambling induces cholesterol redistribution and enables cholesterol depletion in the sperm plasma membrane. J. Cell Sci. 114, 3543–3555.

Flesch, F.M., Wijnand, E., van de Lest, C.H., Colenbrander, B., Van Golde, L.M., Gadella, B.M., 2001b. Capacitation dependent activation of tyrosine phosphorylation generates two sperm head plasma membrane proteins with high primary binding affinity for the zona pellucida. Mol. Reprod. Dev. 60, 107–115.

Foster, L.J., De Hoog, C.L., Mann, M., 2003. Unbiased quantitative proteomics of lipid rafts reveals high specificity for signaling factors. Proc. Natl. Acad. Sci. U.S. A. 100, 5813–5818.

Friend, D.S., 1982. Plasma-membrane diversity in a highly polarized cell. J. Cell Biol. 93, 243–249.

Furimsky, A., Vuong, N., Xu, H., Kumarathasan, P., Xu, M., Weerachatyanukul, W., Bou Khalil, M., Kates, M., Tanphaichitr, N., 2005. Percoll-gradient centrifuged capacitated mouse sperm have increased fertilizing ability and higher contents of sulfogalactosylglycerolipid and docasahexaenoic acid-containing phosphatidylcholine than washed capacitated mouse sperm. Biol. Reprod. 72, 574–583.

Galbiati, F., Razani, B., Lisanti, M.P., 2001. Emerging themes in lipid rafts and caveolae. Cell 108, 403–411.

Hakomori, S., 2000. Cell adhesion/recognition and signal transduction through glycosphingolipid microdomain. Glycoconj. J. 17, 143–151.

Hao, M., Mukherjee, S., Maxfield, F.R., 2001. Cholesterol depletion induces

large scale domain segregation in living cell membranes. Proc. Natl. Acad. Sci. U. S. A. 98, 13072–13077.
Harder, T., 2004. Lipid raft domain and protein networks in T-cell receptor signal transduction. Curr. Opin. Immunol. 16, 353–359.
Harder, T., Simons, K., 1999. Clusters of glycolipid and glycosylphosphatidylinositol-anchored proteins in lymphoid cells: accumulation of actin regulated by local tyrosine phosphorylation. Eur. J. Immunol. 29, 556–562.
Harris, T.J., Siu, C.H., 2002. Reciprocal raft–receptor interactions and the assembly of adhesion complexes. BioEssays 24, 996–1003.
Harrison, R.A., Mairet, B., Miller, N.G., 1993. Flow cytometric studies of bicarbonate-mediated Ca2+ influx in boar sperm populations. Mol. Reprod. Dev. 35, 197–208.
Hedrick, J.L., Wardrip, N.J., 1987. On the macromolecular composition of the zona pellucida from porcine oocytes. Dev. Biol. 121, 478–488.
Horejsi, V., 2003. The roles of membrane microdomains (rafts) in T cell activation. Immunol. Rev. 191, 148–164.
Ipsen, J.H., Karlstrom, G., Mouritsen, O.G., Wennerstrom, H., Zuckermann, M.J., 1987. Phase equilibria in the phosphatidylcholine–cholesterol system. Biochim. Biophys. Acta 905, 162–172.
Iwabuchi, K., Zhang, Y., Handa, K., Withers, D.A., Sinay, P., Hakomori, S., 2000. Reconstitution of membranes simulating "glycosignaling domain" and their susceptibility to lyso-GM3. J. Biol. Chem. 275, 15174–15181.
Kates, M., 1986. Technique of lipidology: isolation, analysis and identification of lipids. In: Burdon, R.H. (Ed.), Laboratory Techniques in Biochemistry and Molecular Biology. Elsevier, New York, pp. 100–278.
Kean, E.L., 1968. Rapid, sensitive spectrophotometric method for quantitative determination of sulfatides. J. Lipid Res. 9, 319–327.
Kerr, C.L., Hanna, W.F., Shaper, J.H., Wright, W.W., 2002. Characterization of zona glycoprotein 3 (ZP3) and ZP2 binding sites on acrosome-intact mouse sperm. Biol. Reprod. 66, 1585–1595.
Laemmli, U.K., 1970. Cleavage of structural proteins during the assembly of the head of bacteriophage T4. Nature 227, 680–685.
London, E., Brown, D.A., 2000. Insolubility of lipids in Triton X-100, physical origin and relationship to sphingolipid/cholesterol membrane domains (rafts). Biochim. Biophys. Acta 1508, 182–195.
Maehashi, E., Sato, C., Ohta, K., Harada, Y., Matsuda, T., Hirohashi, N., Lennarz, W.J., Kitajima, K., 2003. Identification of the sea urchin 350-kDa sperm-binding protein as a new sialic acid-binding lectin that belongs to the heat shock protein 110 family: implication of its binding to gangliosides in sperm lipid rafts in fertilization. J. Biol. Chem. 278, 42050–42057.
Marmor, M.D., Julius, M., 2001. Role for lipid rafts in regulating interleukin-2 receptor signaling. Blood 98, 1489–1497.
McMullen, T.P., Wong, B.C., Tham, E.L., Lewis, R.N., McElhaney, R.N., 1996. Differential scanning calorimetric study of the interaction of cholesterol with the major lipids of the Acholeplasma laidlawii B membrane. Biochemistry 35, 16789–16798.
Melendrez, C.S., Meizel, S., Berger, T., 1994. Comparison of the ability of progesterone and heat solubilized porcine zona pellucida to initiate the porcine sperm acrosome reaction in vitro. Mol. Reprod. Dev. 39, 433–438.
Moffett, S., Brown, D.A., Linder, M.E., 2000. Lipid-dependent targeting of G proteins into rafts. J. Biol. Chem. 275, 2191–2198.
Nagafuku, M., Kabayama, K., Oka, D., Kato, A., Tani-Ichi, S., Shimada, Y., Ohno-Iwashita, Y., Yamazaki, S., Saito, T., Iwabuchi, K., Hamaoka, T., Inokuchi, J.I., Kosugi, A., 2003. Reduction of glycosphingolipid levels in lipid rafts affects the expression state and function of glycosylphosphatidylinositol-anchored proteins, but does not impair signal transduction via the T cell receptor. J. Biol. Chem. 278, 51920–51927.
Nikolopoulou, M., Soucek, D., Vary, J., 1985. Changes in the lipid content of boar sperm plasma membranes during epididymal maturation. Biochim. Biophys. Acta 815, 486–498.
Nishimura, H., Cho, C., Branciforte, D.R., Myles, D.G., Primakoff, P., 2001. Analysis of loss of adhesive function in sperm lacking cyritestin or fertilin beta. Dev. Biol. 233, 204–213.
Ohta, K., Sato, C., Matsuda, T., Toriyama, M., Lennarz, W., Kitajima, K., 1999. Isolation and characterization of low density detergent-insoluble membrane (LD-DIM) fraction from sea urchin sperm. Biochem. Biophys. Res. Commun. 258, 616–623.
Palazzo, A.F., Eng, C.H., Schlaepfer, D.D., Marcantonio, E.E., Gundersen, G.G., 2004. Localized stabilization of microtubules by integrin- and FAK-facilitated Rho signaling. Science 303, 836–839.
Panasiewicz, M., Domek, H., Hoser, G., Kawalec, M., Pacuszka, T., 2003. Structure of the ceramide moiety of GM1 ganglioside determines its occurrence in different detergent-resistant membrane domains in HL-60 cells. Biochemistry 42, 6609–6619.
Parks, J.E., Lynch, D.V., 1992. Lipid composition and thermotropic phase behavior of boar, bull, stallion, and rooster sperm membranes. Cryobiology 29, 255–266.
Peterson, R., Russell, L., Bundman, D., Freund, M., 1980. Evaluation of the purity of boar sperm plasma membranes prepared by nitrogen cavitation. Biol. Reprod. 23, 637–645.
Pike, L.J., 2004. Lipid rafts: heterogeneity on the high sea. Biochem. J. 378, 281–292.
Primakoff, P., Myles, D.G., 2002. Penetration, adhesion, and fusion in mammalian sperm–egg interaction. Science 296, 2183–2185.
Rajendran, L., Masilamani, M., Solomon, S., Tikkanen, R., Stuermer, C.A., Plattner, H., Illges, H., 2003. Asymmetric localization of flotillins/reggies in preassembled platforms confers inherent polarity to hematopoietic cells. Proc. Natl. Acad. Sci. U. S. A. 100, 8241–8246.
Rouquette-Jazdanian, A.K., Pelassy, C., Breittmayer, J.P., Cousin, J.L., Aussel, C., 2002. Metabolic labelling of membrane microdomains/rafts in Jurkat cells indicates the presence of glycerophospholipids implicated in signal transduction by the CD3 T-cell receptor. Biochem. J. 363, 645–655.
Saravanan, K., Shaeren-Wiemers, N., Klein, D., Sandhoff, R., Schwarz, A., Yaghootfam, A., Gieselmann, V., Franken, S., 2004. Specific down-regulation and mistargeting of the lipid raft-associated protein MAL in a glycolipid storage disorder. Neurobiol. Dis. 16, 396–406.
Sato, K., Iwasaki, T., Ogawa, K., Konishi, M., Tokmakov, A.A., Fukami, Y., 2002. Low density detergent-insoluble membrane of *Xenopus* eggs: subcellular microdomain for tyrosine kinase signaling in fertilization. Development 129, 885–896.
Sato, K., Tokmakov, A.A., He, C.L., Kurokawa, M., Iwasaki, T., Shirouzu, M., Fissore, R.A., Yokoyama, S., Fukami, Y., 2003. Reconstitution of Src-dependent phospholipase C gamma phosphorylation and transient calcium release by using membrane rafts and cell-free extracts from *Xenopus* eggs. J. Biol. Chem. 278, 38413–38420.
Schuck, S., Honsho, M., Ekroos, K., Shevchenko, A., Simons, K., 2003. Resistance of cell membranes to different detergents. Proc. Natl. Acad. Sci. U. S. A. 100, 5795–5800.
Shadan, S., James, P.S., Howes, E.A., Jones, R., 2004. Cholesterol efflux alters lipid raft stability and distribution during capacitation of boar spermatozoa. Biol. Reprod. 71, 253–265.
Shao, X., Tarnasky, H.A., Schalles, U., Oko, R., van der Hoorn, F.A., 1997. Interactional cloning of the 84-kDa major outer dense fiber protein Odf84. Leucine zippers mediate associations of Odf84 and Odf27. J. Biol. Chem. 272, 6105–6113.
Shogomori, H., Brown, D.A., 2003. Use of detergents to study membrane rafts: the good, the bad and the ugly. Biol. Chem. 384, 1259–1263.
Silvius, J.R., 2003. Role of cholesterol in lipid raft formation: lessons from lipid model systems. Biochim. Biophys. Acta 1610, 174–183.
Simons, K., Ehehalt, R., 2002. Cholesterol, lipid rafts, and disease. J. Clin. Invest. 110, 597–603.
Simons, K., Vaz, W.L., 2004. Model systems, lipid rafts, and cell membranes. Annu. Rev. Biophys. Biomol. Struct. 33, 269–295.
Sleight, S.B., Miranda, P.V., Plaskett, N.-W., Maier, B., Lysiak, J., Scrable, H., Herr, J.C., Visconti, P.E., 2005. Isolation and proteomic analysis of mouse sperm detergent-resistant membrane fractions. Evidence for dissociation of lipid rafts during capacitation. Biol. Reprod. 73, 721–729.
Stulnig, T.M., Huber, J., Leitinger, N., Imre, E.M., Angelisova, P., Nowotny, P., Waldhausl, W., 2001. Polyunsaturated eicosapentaenoic acid displaces proteins from membrane rafts by altering raft lipid composition. J. Biol. Chem. 276, 37335–37340.
Tanphaichitr, N., Moase, C., Taylor, T., Surewicz, K., Hansen, C., Namking, M., Berube, B., Kamolvarin, N., Lingwood, C., Sullivan, R., Rattanachaiyanont, M., White, D., 1998. Isolation of antiSLIP1-reactive boar sperm

P68/62 and its binding to mammalian zona pellucida. Molec. Reprod. Dev. 49, 203–216.

Tanphaichitr, N., Bou Khalil, M., Weerachatyanukul, W., Kates, M., Xu, H., Carmona, E., Attar, M., Carrier, D., 2003. Physiological and biophysical properties of male germ cell sulfogalactosylglycerolipid. In: De Vries, S. (Ed.), Lipid Metabolism and Male Fertility. AOCS Press, Champaign, IL, pp. 125–148.

Tardiff, S., Dube, C., Chevalier, S., Bailey, J.L., 2001. Capacitation is associated with tyrosine phosphorylation and tyrosine kinase-like activity of pig sperm proteins. Biol. Reprod. 65, 784–792.

Towbin, H., Gordon, J., 1984. Immunoblotting and dot immunobinding-current status and outlook. J. Immunol. Methods 72, 313–340.

Travis, A.J., Merdiushev, T., Vargas, L.A., Jones, B.H., Purdon, M.A., Nipper, R.W., Galatioto, J., 2001. Expression and localization of caveolin-1, and the presence of membrane rafts, in mouse and guinea pig spermatozoa. Dev. Biol. 240, 599–610.

Tupper, S., Wong, P.T.T., Kates, M., Tanphaichitr, N., 1994. Interaction of divalent cations with germ cell specific sulfogalactosylglycerolipid and the effects on lipid chain dynamics. Biochemistry 33, 13250–13258.

van Gestel, R.A., Brewis, I.A., Ashton, P.R., Helms, J.B., Brouwers, J.F., Gadella, B.M., 2005. Capacitation-dependent concentration of lipid rafts in the apical ridge head area of porcine sperm cells. Mol. Human Reprod. 11, 583–590.

Visconti, P.E., Westbrook, V.A., Chertihin, O., Demarco, I., Sleight, S., Diekman, A.B., 2002. Novel signaling pathways involved in sperm acquisition of fertilizing capacity. J. Reprod. Immunol. 53, 133–150.

Wassarman, P.M., 2005. Contribution of mouse egg zona pellucida glycoproteins to gamete recognition during fertilization. J. Cell. Physiol. 204, 388–391.

Weerachatyanukul, W., Rattanachaiyanont, M., Carmona, E., Furimsky, A., Mai, A., Shoushtarian, A., Sirichotiyakul, S., Ballakier, H., Leader, A., Tanphaichitr, N., 2001. Sulfogalactosylglycerolipid is involved in human gamete interaction. Mol. Reprod. Dev. 60, 569–578.

White, D., Weerachatyanukul, W., Gadella, B., Kamolvarin, N., Attar, M., Tanphaichitr, N., 2000. Role of sperm sulfogalactosylglycerolipid in mouse sperm–zona pellucida binding. Biol. Reprod. 63, 147–155.

Wolf, D., Hagopian, S., Ishijima, S., 1986. Changes in sperm plasma membrane lipid diffusibility after hyperactivation during in vitro capacitation in the mouse. J. Cell Biol. 102, 1372–1377.

Wong, P.T.T., Mantsch, H.H., 1988. High-pressure infrared spectroscopic evidence of water binding sites in 1,2-diacylphospholipids. Chem. Phys. Lipids 46, 213–224.

Xu, X., Bittman, R., Duportail, G., Heissler, D., Vilcheze, C., London, E., 2001. Effect of the structure of natural sterols and sphingolipids on the formation of ordered sphingolipid/sterol domains (rafts). J. Biol. Chem. 276, 33540–33546.

Yanagimachi, R., 1994. Mammalian fertilization. In: Knobil, E. (Ed.), The Physiology of Reproduction. Raven Press Ltd., New York, NY, pp. 189–317.

Yurewicz, E.C., Sacco, A.G., Subramanian, M.G., 1987. Structural characterization of the M_r = 55,000 antigen (ZP3) of porcine oocyte zona pellucida. J. Biol. Chem. 262, 564–571.

Yurewicz, E.C., Pack, B.A., Armant, D.R., Sacco, A.G., 1993. Porcine zona pellucida ZP3 à glycoprotein mediates binding of the biotin-labeled M{-r} 55,000 family (ZP3) to boar sperm membrane vesicles. Mol. Reprod. Dev. 36, 382–389.

Yurewicz, E.C., Sacco, A.G., Gupta, S.K., Xu, N., Gage, D.A., 1998. Hetero-oligomerization-dependent binding of pig oocyte zona pellucida glycoproteins ZPB and ZPC to boar sperm membrane vesicles. J. Biol. Chem. 273, 7488–7494.